RELATIVE APPARENT MOLAL HEAT CONTENTS OF SOME

AQUEOUS RARE-EARTH CHLORIDE SOLUTIONS AT 25°C

by

George William Pepple

A Dissertation Submitted to the

Graduate Faculty in Partial Fulfillment of

The Requirements for the Degree of

DOCTOR OF PHILOSOPHY

Major Subject: Physical Chemistry

Approved:

Signature was redacted for privacy.

In Charge of Major Work

Signature was redacted for privacy.

Head of Major Department

Signature was redacted for privacy.

Dean of Graduate College

Iowa State University
Of Science and Technology
Ames, Iowa

1967

TABLE OF CONTENTS

I. INTRODUCTION

The study of water and aqueous solutions has long played a significant role in the development of chemistry. The emergence of physical chemistry as a separate discipline occurred with the formation of _Zeitschrift fur Physikalische Chemie_ in 1887 and for the next 30 years this journal was concerned mainly with solution chemistry studies.

Electrolytic solutions are very complex systems and in spite of such a long and intensive interest in the subject a complete theoretical understanding of any but the most dilute electrolytic solutions remains one of the major unsolved problems of physical chemistry.

The electrolytic solution theory of Debye and Hückel (3) predicts the limiting behaviour of the thermodynamic properties of solutions of strong electrolytes. Due to a number of simplifying assumptions in the model and in the mathematical treatment, the Debye-Hückel theory (3) becomes conceptually valid only in the limit of infinite dilution of the solute. Attempts to modify some of the assumptions and thereby extend the range of the Debye-Hückel theory have in general met with limited success.

Heats of dilution of solutions of a number of electrolytes have been accurately measured into concentration ranges where the Debye-Hückel limiting behaviour is apparently being followed. The results from several studies of univalent

electrolytes are in quantitative agreement with the Debye-
Hückel predictions (24, 64). The situation is more complex with
higher valent electrolytes, however, and the results do not
generally agree as well with the theoretical predictions (34,
42, 46, 64). The thermodynamic properties of electrolytic so-
lutions are proportional to the sum of the squares of the ionic
charges and as a consequence the deviations from the theoreti-
cal limiting law become significant much sooner for divalent
and trivalent electrolytes than for univalent electrolytes.
Part of the results of this thesis are concerned with the be-
haviour of the heats of dilution of several aqueous rare-earth
chlorides at very low concentrations.

Because of their unique electronic configurations lanthanum
and the rare-earths constitute a series of elements whose
chemical properties are very much alike. Their chemical be-
haviour is determined by the three valence electrons common to
all of them. As the atomic number increases across the series
the additional electrons go into the 4f subshell. The 4f
subshell is shielded by the filled 5s and 5p subshells which
explains why the 4f electrons influence the chemical behaviour
of the rare-earths to such a relatively small extent.

Rare-earths are now available in kilogram quantities in
very high purity from the large scale ion exchange processes
developed at Ames Laboratory (41). This laboratory has under-
taken an extensive study of the thermodynamic and transport
properties of aqueous rare-earth solutions from infinite

dilution to saturation (4, 49, 50, 51, 51a, 52, 53). The rare-earths are an excellent group of elements with which to study solution properties as a function of ionic radii. The rare-earths exist in aqueous solution as tripositive ions. Unlike other trivalent cations they show little tendency to form strong association complexes with the simple anions. Likewise their tendency to hydrolyze is comparatively small and can be controlled. The rare-earth salts of many of the common anions are appreciably soluble in water.

Thermodynamics is the science which mathematically treats the relationships between heat and work. It is an exact science and its rules hold for all systems. From a statistical point of view thermodynamic properties are the averages of extremely large numbers of atomic level events. If the atomic behaviour of a system is sufficiently well known its thermodynamic behaviour can be accurately predicted. In a system as complex as an electrolytic solution a number of separate but interdependent events contribute to the thermodynamic values. The Debye-Hückel theory (3) is successful on the basis that as solutions become sufficiently dilute the contributions of the various ion-solvent interactions become negligible and the solution thermodynamic properties are determined solely by the long range electrical interactions between the ions. Thus, at concentrations above the Debye-Hückel limiting law range, a detailed knowledge of the ion-solvent interactions and structure in an electrolytic solution is a prerequisite to the prediction

of its thermodynamic properties. It is rarely possible to proceed with complete certainty in the opposite direction and predict atomic level behaviour from thermodynamic values. However, if a sufficient variety of thermodynamic properties have been determined for a given system it is often possible from a comparison of these properties to draw reasonably definite conclusions as to the presence or absence of certain interactions. Such speculations often suggest, and are often supported by, independent experimental evidence such as structural or spectroscopic studies.

Heats of dilution measure energy changes due to complex dissociation, hydrolysis, hydration, modification of the solvent by the hydrated ions, and electrical work which accompany dilution. Heats of dilution are valuable in solution chemistry because they are needed to correct any reaction involving an electrolyte to its standard state which is usually infinite dilution.

This thesis is a report of the measurement of the heats of dilution of $NdCl_3$, $SmCl_3$, $EuCl_3$, $GdCl_3$, $DyCl_3$, $ErCl_3$, $TmCl_3$, and $LuCl_3$ in aqueous solutions from infinite dilution to saturation. The heats of solution of $LaCl_3 \cdot 7H_2O$, $PrCl_3 \cdot 7H_2O$, $NdCl_3 \cdot 6H_2O$, $SmCl_3 \cdot 6H_2O$, $EuCl_3 \cdot 6H_2O$, $GdCl_3 \cdot 6H_2O$, $DyCl_3 \cdot 6H_2O$, $ErCl_3 \cdot 6H_2O$, $TmCl_3 \cdot 6H_2O$, $YbCl_3 \cdot 6H_2O$, and $LuCl_3 \cdot 6H_2O$ were also measured. The relative partial molal heat contents were calculated from the heat of dilution data and were in turn combined with activity data to calculate the partial molal excess

entropies of dilution. These measurements plus those of DeKock
(4) account for the heats of dilution of thirteen rare-earth
chlorides. Studies of the partial molal volumes (53), viscosi-
ties (52), and heat capacities (51a) of some aqueous rare-earth
chlorides indicate that a hydration change takes place across
the middle portion of the rare-earth series and it was of
interest to see how the trend in the heats of dilution would
correlate with the trends in the other properties. These
heats of dilution and the other properties of the aqueous
rare-earth chlorides will provide a stringent test for any new
theories of electrolytic solutions.

II. THEORY

The physical chemistry of dilute electrolytic solutions has had a firm theoretical basis since 1923 when Debye and Hückel (3) published their well known theory of electrolytic solutions.

The Debye-Hückel theory predicts the behaviour of the excess free energy of electrolytic solutions. The excess free energy is the free energy which an electrolytic solution has above that of an analogous ideal nonelectrolytic solution. Other excess thermodynamic functions can be derived from the excess free energy by differentiation with respect to the appropriate variables.

The Debye-Hückel theory is based on the following postulates:

1. Strong electrolytes are completely dissociated into ions in solution.

2. All deviations from ideality are attributed to the electrostatic interactions of the ions.

3. The ions are rigid spheres with a mean distance of closest approach.

4. The solvent is a continuous medium with a uniform dielectric constant. For dilute solutions the bulk dielectric constant of the pure solvent is used.

5. In the absence of external fields there is a spherically symmetric distribution of ions about any given

ion commensurate with the condition of electro-
neutrality, and thus containing on the average more
ions of unlike charge than like charge. The time
average of this distribution is given by the Boltzmann
distribution function.

6. The electrostatic potential at any point in the so-
   lution can be calculated using the Poisson equation
   and a form of the Boltzmann distribution function
   compatible with the linear superposition of fields.

Starting from these assumptions Debye and Hückel derived
equation 2.1 as an expression of the excess free energy of a
solution per mole of solute. Equations 2.2 and 2.3 define the
functions Υ and (Ka).

$$\overline{F}(ex) = vNkT\ln(f\underline{+}) = -\sum_i v_i z_i^2 \epsilon^2 \frac{NKT(Ka)}{D} \tag{2.1}$$

$$K = \left[\sum v_i z_i^2\right]^{1/2} \left[\frac{4\pi N\epsilon^2}{1000\ DkT}\right]^{1/2} c^{1/2} \tag{2.2}$$

$$\Upsilon(Ka) = \left[\frac{1}{Ka}\right]^3 \left[\ln(1 + Ka) - Ka + \frac{(Ka)^2}{2}\right] \tag{2.3}$$

The symbols in the previous equations have the following
meanings:

  $f\underline{+}$ = excess molar free energy of the solute

  v = total number of ions obtained from one mole of solute

  v_i = number of ions of charge z_i obtained from one mole of
   solute

  ϵ = fundamental electronic charge

  N = Avogadro's number

k = Boltzmann's constant

D = dielectric constant of the pure solvent

T = absolute temperature

c = molar concentration of the solute

a = mean distance of closest approach of the ions

$$\lim_{c \longrightarrow 0} Ka = 0 \tag{2.4}$$

$$\lim_{c \longrightarrow 0} \Upsilon(Ka) = 1 \tag{2.5}$$

Equations 2.4 and 2.5 hold in the limit of infinite dilution. Using them, equation 2.1 can be written in the form of the Debye-Hückel limiting law for the activity coefficient, equations 2.6 and 2.7.

$$\frac{\overline{F}(ex)}{NkT} = \ln(f\underline{\pm}) = -\sum_i \frac{1}{v} \left[\frac{v_i z_i^2}{DkT}\right]^{3/2} \left[\frac{4\pi N\epsilon^6}{1000}\right] c^{1/2} \tag{2.6}$$

$$\frac{\overline{F}(ex)}{NkT} = \ln(f\underline{\pm}) = -A_f c^{1/2} \tag{2.7}$$

The limiting law expression is often written in terms of the ionic strength I, defined in equation 2.9.

$$\ln(f\underline{\pm}) = A_f' I^{1/2} \tag{2.8}$$

$$I = \sum_i \frac{c_i z_i^2}{2} \tag{2.9}$$

The excess enthalpy of dilution of the solute can be

obtained from equation 2.1 through use of the Gibbs-Helmholtz relationship, equation 2.10.

$$\frac{d\left[\frac{F}{T}\right]}{dT} = \frac{-H}{T^2} \tag{2.10}$$

The partial molal enthalpy of a component of an ideal solution is independent of its concentration; an ideal solution has no enthalpy of dilution. Therefore the excess enthalpy of dilution is represented by $\emptyset_L$, the total enthalpy of dilution per mole of solute,

$$\emptyset_L = -A\left[\frac{1}{1+Ka}\left(\frac{dlnD}{dT} + \frac{1}{T}\right) + \frac{\sigma\alpha}{3}\right]c^{1/2} + A\left[\sigma - \frac{1}{1+Ka}\right]$$

$$\left[\frac{dlna}{dT}\right]c^{1/2} \tag{2.11}$$

where α is the thermal expansibility of the solvent and the functions σ and A are defined by the following equations.

$$\sigma = \left[\frac{1}{Ka}\right]^3\left[1 + Ka - \frac{1}{1+Ka} - 2ln(1+Ka)\right] \tag{2.12}$$

$$A = NkT^2\left[\frac{\pi N\epsilon^6}{1000 \ (DkT)^3}\right]^{1/2}\left[\sum_i v_i z_i^2\right]^{3/2} \tag{2.13}$$

In the limit of infinite dilution the expression for the enthalpy of dilution reduces to the following form.

$$\emptyset_L = -A\left[\frac{dlnD}{dT} + \frac{1}{T} + \frac{\alpha}{3}\right]c^{1/2} \tag{2.14}$$

$$\emptyset_L = A_H c^{1/2} \qquad\qquad (2.15)$$

At high dilutions the molar concentration (moles solute per 1000 milliliters solution) is approximately equal to the molal concentration (moles solute per 1000 grams solvent). In terms of molal concentrations,

$$\emptyset_L = A_H m^{1/2} \qquad\qquad (2.16)$$

The constant A_H, the theoretical limiting slope of the enthalpy curve, is quite sensitive to small uncertainties in the terms in the parentheses in equation 2.14. This is because, for water, the $d\ln D/dT$ term is negative and not much larger than the sum of the other two terms. Harned and Owen (27) evaluate A_H to be 6925 for aqueous 3-1 electrolytes at 25°C. from the data of Wyman and Ingalls (62) for the dielectric constant of water as a function of temperature and from the values of the density of water given in the "International Critical Tables" (58b).

All extensions of the Debye-Huckel limiting theory for the behaviour of solute activity coefficients have been put forth with the introduction of one or more non-fundamental parameters. Such extension can lead to expressions capable of representing the activity coefficients of particular solutes to moderate concentrations. However, since the temperature and

pressure derivatives of the parameters are generally unknown, these extensions have been of little value in predicting the behaviour of the excess thermodynamic quantities derived from the activity coefficients. For example, in the preceding derivation of the dilution enthalpy the temperature dependence of the a-parameter is not known and so only the limiting behaviour of $\emptyset_L$ can be predicted.

A large number of works treating the Debye-Hückel theory have been published. The following cited references represent some of the better known and more successful treatments. Bjerrum (1) and Fuoss and Krauss (15, 16) took into account the effects of ion association. Scatchard (47), Hückel (29), Stokes and Robinson (54), and Glueckauf (17) considered solvent-solute interactions. Gronwall, LaMer, and Greiff (21), Eigen and Wicke (7, 60), and Guggenheim (23) undertook extended treatments of the Poisson-Boltzmann equation. Kramers (33), Fowler (10), Onsager (38), Kirkwood (31), Fowler and Guggenheim (11), and Kirkwood and Poirier (32) examined the statistical mechanical basis of the Debye-Hückel theory. The Debye-Hückel theory, and electrolytic solution chemistry in general, are covered in the treatises of Harned and Owen (27) and Robinson and Stokes (43).

The functional form of the Debye-Hückel limiting law is generally accepted. An adequate theory for concentrated electrolytes is contingent upon a better understanding of the short-range interactions taking place in electrolytic solutions.

III. THERMODYNAMICS

The first law of thermodynamics defines the relationship between heat q, work w, and internal energy E.

$$\Delta E = q + w \tag{3.1}$$

The usual convention of labeling as positive the energy changes due to heat absorbed by or work done on a system is followed throughout this treatise. When no external fields are present and only mechanical work is performed on a system equation 3.1 can be written in the form of equation 3.2, where p and V stand respectively for the pressure and volume of the system.

$$\Delta E = q - \Delta(pV) \tag{3.2}$$

The enthalpy H is defined by a rearrangement of equation 3.2. For the particular case of a constant pressure process the enthalpy change of a system is given by equation 3.3.

$$\Delta H = \Delta E + p\Delta V \tag{3.3}$$

This equation is of particular usefulness to thermochemists since many reactions are carried out under conditions of constant pressure.

All thermodynamic functions are state functions. A function of state has the important property that its value depends only upon the state of a system and not upon how the state was reached. This is equivalent to saying that the derivative of a state function is an exact differential. The definite integral of an exact differential depends only upon the limits of the integral and not upon the path over which the

integration is carried out. Energy, pressure, and volume are typical state functions. Enthalpy is also a state function since it is defined in terms of state functions. Changes in q and w depend upon the path taken between states and q and w are therefore not state functions.

Thermodynamic properties are either intensive or extensive functions. The distinction between these two types is that extensive functions, such as energy or volume, are dependent upon the mass of the system while intensive functions, such as temperature or molar volume, are independent of the mass of the system. Rigorously, an extensive thermodynamic function is defined to be homogeneous of first order in the number of moles of material present in the system while the intensive variables are being held constant. This means that if G is an extensive function,

$$G \ (T, \ P, \ n_1, \ n_2, \ ..., \ n_j) \tag{3.4}$$

then multiplying each of the mole numbers n_j by a factor increases the value of G by the same factor.

$$\beta \ G = G \ (T, \ P, \ \beta n_1, \ \beta n_2, \ ..., \ \beta n_j) \tag{3.5}$$

According to Euler's theorem of homogeneous functions G can be represented by equation 3.6, where the subscripts T, P, n_j imply that these quantities are held constant during the differentiation.

$$G = \sum_i n_i \left(\frac{G}{n_i}\right)_{T, P, n_j} \tag{3.6}$$

$$\overline{G}_i = \left(\frac{G}{n_i}\right)_{T, P, n_j} \tag{3.7}$$

The quantity $\overline{G}_i$ in equation 3.7 is called the partial molal G of component i at constant temperature and pressure. Physically, $\overline{G}_i$ can be imagined to be the total change in G when one mole of component i is added to an infinite amount of the system.

This research was concerned with the measurement of the heat absorbed or evolved upon dilution of a rare-earth chloride solution or upon solution of a rare-earth chloride hydrate crystal. All systems studied were two-component rare-earth chloride-water systems. The experiments were carried out at constant pressure and composition. Under these conditions the measured heats were enthalpies.

Referring to equation 3.6, the enthalpy of a two-component system can be given by the following expression, where the subscript 1 refers to the solvent water and the subscript 2 refers to the solute rare-earth chloride.

$$H^i (n_1, n_2) = n_1 \overline{H}_1^i + n_2 \overline{H}_2^i \tag{3.8}$$

The superscript i refers to the state of the solution. The quantities $\overline{H}_1$ and $\overline{H}_2$ are called the partial molar enthalpies or, more commonly, the partial molar heat contents of the

solvent and solute respectively.

Solution thermodynamic functions are customarily expressed with respect to the solvent standard state of pure solvent and with respect to the hypothetical one-molal ideal solute standard state. The enthalpy of a two-component system in its standard state is given by equation 3.9, with the superscript o indicating standard state conditions.

$$H^O (n_1, n_2) = n_1\bar{H}_1^O + n_2\bar{H}_2^O \tag{3.9}$$

The enthalpy of a two-component system in state i is given with respect to its standard state enthalpy by the following equation.

$$H^i - H^O = n_1(\bar{H}_1^i - \bar{H}_1^O) + n_2(\bar{H}_2^i - \bar{H}_2^O) \tag{3.10}$$

The relative partial molar heat content $\bar{L}_j$ is defined to be the difference in enthalpy for some component j between its state i in the solution and its standard state.

$$\bar{L}_j^i = \bar{H}_j^i - \bar{H}_j^O \tag{3.11}$$

Equation 3.10 can be conveniently expressed in terms of relative heat contents.

$$L^i (n_1, n_2) = n_1\bar{L}_1^i + n_2\bar{L}_2^i \tag{3.12}$$

The apparent molar function of a thermodynamic property G is defined by the following expression.

$$\phi_G^i = \frac{G^i(n_1, n_2) - n_1 \bar{G}_1^o}{n_2} \tag{3.13}$$

The relative apparent molar heat content ϕ_L is the enthalpy of dilution of a solution per mole of solute.

$$\phi_L^i = \frac{L^i(n_1, n_2) - n_1 \bar{L}_1^o}{n_2} \tag{3.14}$$

It is obvious that $\bar{L}_1^o$, the relative partial molar heat content of the pure solvent, is identically zero. Using the Raoults law standard state for component 1,

$$\bar{L}_1^o = \bar{H}_1^o - \bar{H}_1^o \tag{3.15}$$

The relative apparent molar heat content is an extremely useful function because it relates the defined partial molar functions (equation 3.12) to the experimentally observed enthalpies of dilution. The following expression is obtained by combining equations 3.12 and 3.14.

$$n_2 \phi_L^i = L^i(n_1, n_2) = n_1 \bar{L}_1^i + n_2 \bar{L}_2^i \tag{3.16}$$

Expressions for the relative partial molar heat contents are derived from equation 3.16 by differentiation and substitution.

$$\bar{L}_2 = \frac{\partial L}{\partial n_2} = n_2 \left[\frac{\partial \phi_L}{\partial n_2} \right]_{T,P,n.} + \phi_L \tag{3.17}$$

$$\bar{L}_1 = \frac{n_2 \phi_L - n_2 \bar{L}_2}{n_1} = \frac{-n_2^2}{n_1} \left[\frac{\partial \phi_L}{\partial n_2} \right]_{T,P,n.} \tag{3.18}$$

The molality concentration scale was used throughout this research. Equations 3.19 and 3.20, where M is the molecular weight of the solvent, are identities for conversion between molality and mole number concentration scales.

$$n_2 = m \tag{3.19}$$

$$n_1 = \frac{1000}{M} \tag{3.20}$$

The concentration dependence of $\emptyset_L$ is expressed in terms of the square root of the molality since this is the functional behaviour predicted by the Debye-Hückel limiting law (3). The following two equations express the relative partial molal heat contents in terms of the square root of the molality.

$$\overline{L}_2 = \frac{m^{1/2}}{2} \frac{\partial \emptyset_L}{\partial m^{1/2}} + \emptyset_L \tag{3.21}$$

$$\overline{L}_1 = - \frac{m^{3/2}}{2000} \frac{\partial \emptyset_L}{\partial m^{1/2}} \tag{3.22}$$

Assume that a solution containing n_1 moles of water and n_2 moles of rare-earth chloride is diluted into n_1^* moles of pure water. The relative heat content of the system before the dilution is given by equation 3.23,

$$L^i(n_1, n_2) = n_1 \overline{L}_1^i + n_2 \overline{L}_2^i + n_1^* \overline{L}_1^o \tag{3.23}$$

and the relative heat content of the system after the dilution is given by equation 3.24.

$$L^f(n_1,n_2) = (n_1 + n_1^*)\bar{L}_1^f + n_2\bar{L}_2^f \tag{3.24}$$

The difference in the heat content between the initial and final states is the enthalpy of dilution.

$$\Delta H_{dil.} = (n_1 + n_1^*)\bar{L}_1^f + n_2\bar{L}_2^f - n_1\bar{L}_1^i - n_2\bar{L}_2^i \tag{3.25}$$

Referring to equation 3.16, the expression for the enthalpy of dilution can be written in terms of the relative apparent molal heat contents.

$$\Delta H_{dil.} = n_2\emptyset_L^f - n_2\emptyset_L^i \tag{3.26}$$

If the relative apparent molal heat content of the final solution is known it can be combined with the enthalpy of dilution to determine the relative apparent molal heat content of the initial solution. The quantity ΔH_D is the enthalpy of dilution per mole of solute.

$$\emptyset_L^i = \emptyset_L^f - \Delta H_D \tag{3.27}$$

Assume that n_2 moles of rare-earth chloride hydrate crystals are dissolved in n_1 moles of water. The relative heat content of the initial system is given by equation 3.28,

$$L^i(n_1,n_2) = n_2\bar{L}^{\cdot} + n_1\bar{L}_1^o \tag{3.28}$$

and the relative heat content of the final system is given by equation 3.29,

$$L^f(n_1, n_2) = (n_1 + n_1^*)\bar{L}_1^f + n_2\bar{L}_2^f \qquad (3.29)$$

where $\bar{L}\cdot$ is the relative molar heat content of the rare-earth chloride hydrate and n_1^* is the number of moles of water in the hydrate sample. The difference in the relative heat contents between the initial and final states is the enthalpy of solution to the final state.

$$\Delta H_{sol.} = (n_1 + n_1^*)\bar{L}_1^f + n_2\bar{L}_2^f - n_2\bar{L}\cdot \qquad (3.30)$$

The expression for the enthalpy of solution can be simplified using equation 3.16.

$$\Delta H_{sol.} = n_2\phi_L^f - n_2\bar{L}\cdot \qquad (3.31)$$

Since ϕ_L goes to zero at infinite dilution a study of the enthalpy of solution of a crystal versus the final solution concentration can give values for both the relative apparent apparent molal heat content of the solution and the relative molar heat content of the crystal. For the case of the rare-earth chlorides, however, $\bar{L}\cdot$ is much larger than ϕ_L, particularly for low final concentrations, and the uncertainties in the measured heat of solution values contribute serious relative errors to the ϕ_L^f values. A more satisfactory use of the heat of solution data is to combine it with ϕ_L^f values from enthalpy of dilution studies to obtain the relative molar heat contents of the crystal,

$$L \cdot = \emptyset_L{}^f - \Delta H_S \qquad (3.32)$$

where H_S is the molar enthalpy of solution of the crystal.

IV. EXPERIMENTAL APPARATUS

All heat measurements performed in this research were
carried out on a differential adiabatic solution calorimeter.
This calorimeter was constructed by Naumann (37) and was modeled
after an apparatus designed by Gucker, Pickard, and Planck (22).
Modifications have since been introduced into the apparatus by
Eberts (5), Csejka (2), and DeKock (4). Further improvements
were made in the apparatus during the course of this research,
the most important of which were rebuilding the submarine (adi-
abatic heat shield) and submarine lid, and designing and
building a new system for suspending the calorimeter container
lids and supporting the calorimeter containers. These changes
increased the reliability of the apparatus and lowered the
probability of random leaks. The design and operation of a
number of types of calorimeters are treated by Swietoslawski
(56), White (59), Sturtevant (55), and Skinner (48).

A schematic design of the calorimeter is given in Figure
1, and of the electrical circuits in Figures 2 and 3. Refer-
ence to the figures will be designated (i-X) where i refers to
the figure and X to the alphabetically labeled parts.

The adiabatically controlled water bath was a 22-gallon
double-walled cylindrical container. The copper walls were
separated by 3 inches of exploded mica insulation. Cooling
coils (1-A) and an auxiliary 500-watt Calrod heater passed
through the walls into the water bath. The water bath was
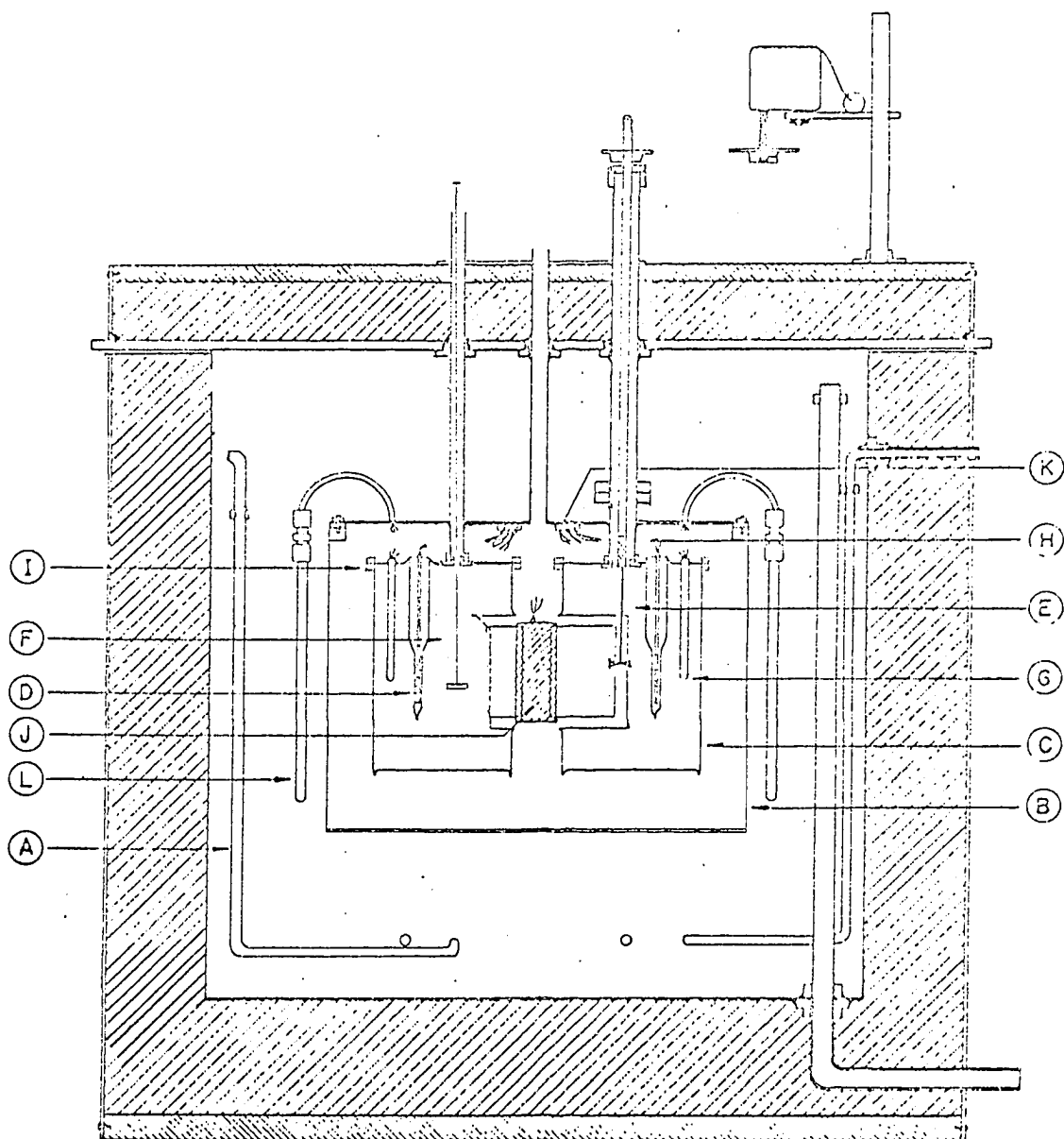
Figure 1. Adiabatic differential calorimeter.
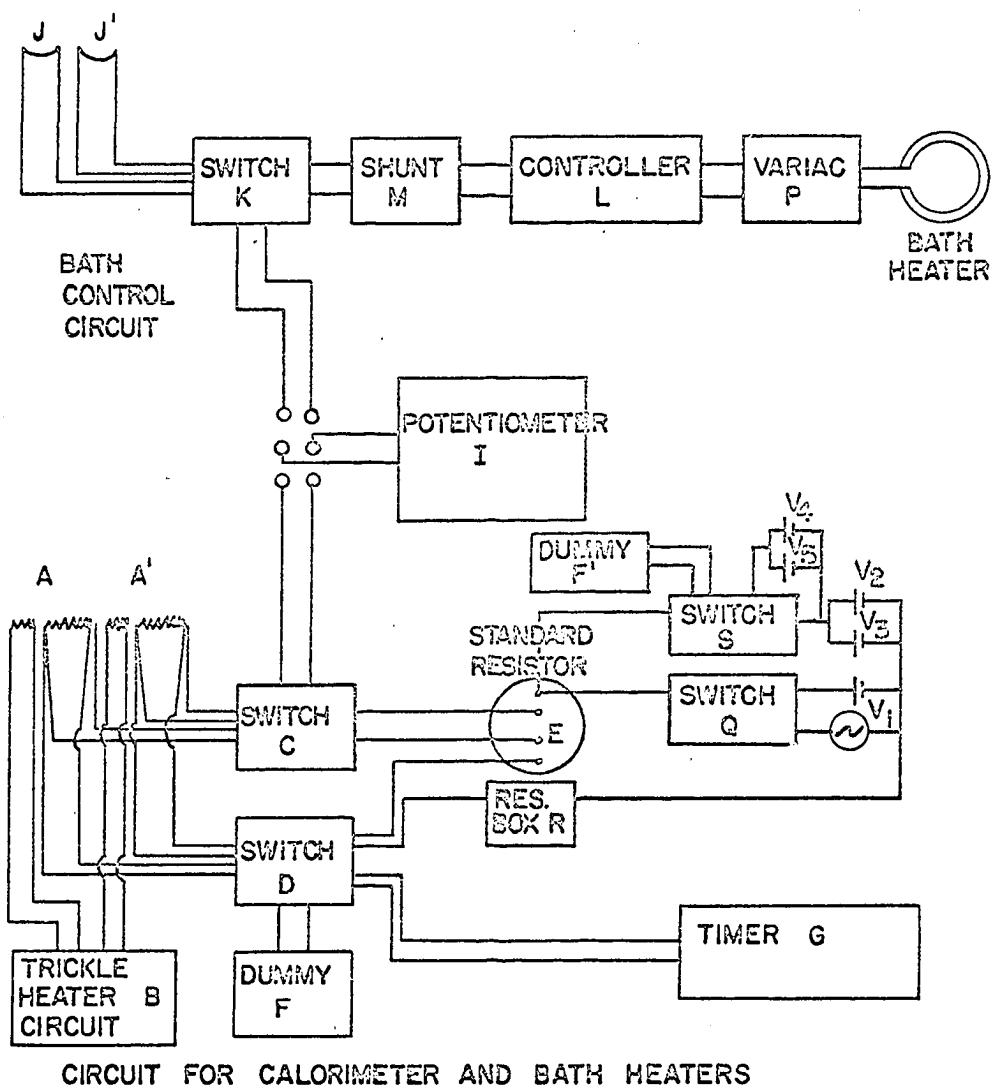
Figure 2. Schematic diagram of calorimeter circuits.
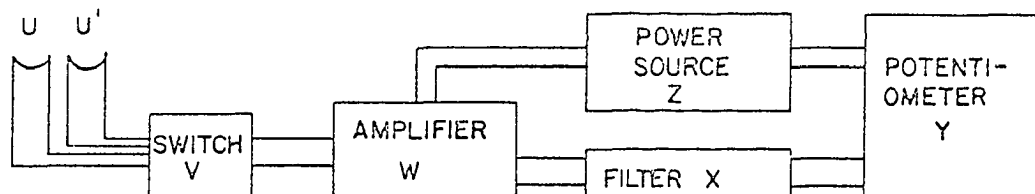
CIRCUIT FOR MAIN THERMEL
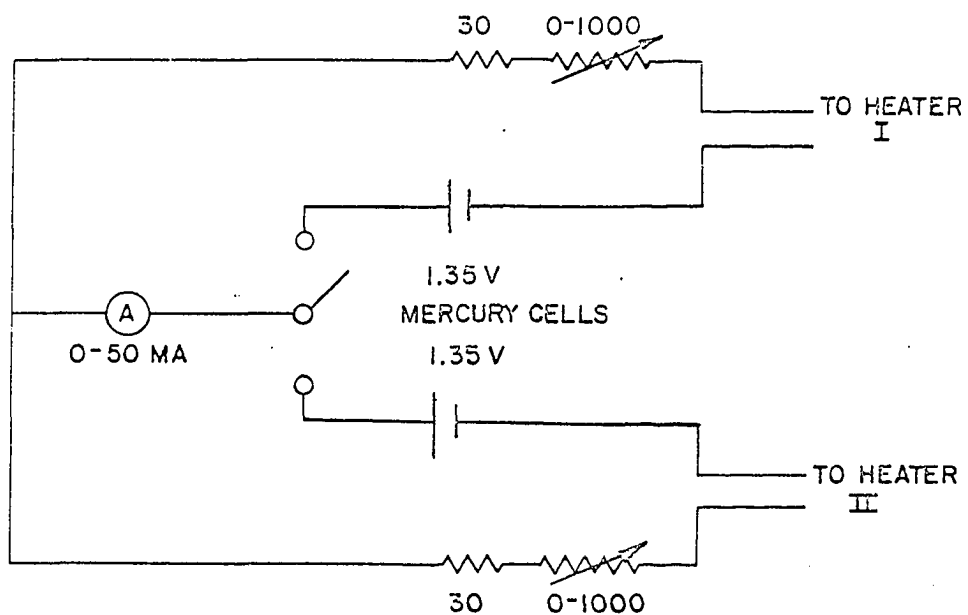
CURRENT SOURCE FOR TRICKLE HEATERS

Figure 3. Schematic diagram of thermopile and trickle heater circuits.

mounted on a moveable base. The bath could be raised with a
hydraulic jack to the level of the water bath lid, which rested
4-1/2 feet above the floor on a rigid angle-iron frame.

Excellent stirring in the water bath was achieved with a
centrifugal stirrer (Central Scientific Company Calalog number
18850). The stirrer directed the water downward, across the
submarine lid, toward a copper baffle which helped reduce
thermal gradients in the water by introducing turbulent flow.

A 500-watt Calrod heater which encircled the submarine and
was used to maintain adiabatic temperature control was suspended
from the water bath lid.

The apparatus was located in a room thermostated between
23.5 and 25.0°C.

An adiabatic heat shield, the submarine, provided a water-
tight enclosure for the calorimeter containers and insulated
them from the relatively large and rapid temperature oscil-
lations of the water bath. The submarine was 12-1/2 inches
long by 7 inches wide by 8-3/4 inches deep with parallel sides
and semicircular ends. The sides were constructed from 1/8-
inch monel sheet and the bottom was constructed from 1/4-inch
monel sheet. All seams were arc-welded to provide permanent
integrity against leaks. A 1/4-inch by 1/4-inch inconel strip
welded to the upper inside edge of the submarine wall held
twenty countersunk machine screws used to attach the submarine
to its lid. An 1/8-inch rubber O-ring rested on this strip,
inside the screws, and provided a water tight seal between the

submarine and its lid.

The submarine lid was a 1/4-inch monel plate with twenty holes drilled around its circumference to accommodate the machine screws from the submarine. Eight brass tubes and two copper tubes, which housed the stirrer shafts, sample holder rods, and electrical leads from the calorimeter containers, were silver soldered into the holes in the submarine lid. The eight brass tubes passed through collars threaded into the water bath lid. The submarine lid was suspended eight inches below the water bath lid (seven inches below the water level) by the brass tubes which were secured in the collars with set screws.

The calorimeter containers (1-C) were constructed from 15-mil tantalum sheet. Each container had a cylindrical shape, 4 inches in diameter by 6 inches high. A rectangular well, 5/16-inch wide by 3-3/8 inches deep by 2-1/4 inches high, to accommodate the main thermopile (1-J), was welded into the side of each container. A 1/4-inch rim was spun outward at a 90° angle on the top of each container. Eight machine screws mounted on a 1/4-inch by 1/8-inch brass ring passed, from beneath, through matching holes in a container rim, a container lid, and another 1/4-inch by 1/8-inch brass ring. When the system was bolted together the eight machine screws held each calorimeter container securely to its lid (1-I). A thin coat of a viscous grease (Apiezon L grease) on the container rims insured a vapor tight seal.

The calorimeter container lids were constructed from 30-mil tantalum sheet. Each lid had eight holes drilled around its circumference to match the holes in a container rim. A 1/2-inch diameter by 4-3/4 inch tantalum tube (1-D) was welded into each lid to provide a housing for the calorimeter heaters. Another tantalum tube (1-G), 1/4-inch in diameter by 3-1/4 inches, was welded into each lid to hold one end of a control thermopile. A stirrer shaft (1-E) and a sample holder rod (1-F) passed respectively through 1/2-inch and 5/16-inch holes in the container lids.

A calorimeter container lid was suspended from the submarine lid by two thin-walled stainless steel tubes (1-H). The stainless steel tubes were silver soldered at the top to the submarine lid and at the bottom to brass flanges. Machined brass lugs screwed into the flanges (through holes in the lids) and provided support for the lids. Thin teflon gaskets coated with Apiezon grease provided vapor tight seals. The larger stainless steel tube (10-mil, 1/2-inch diameter) was situated over the 1/2-inch hole and the smaller tube (6-mil, 5/16-inch diameter) was situated over the 5/16-inch hole in each lid. The stainless steel tubes were 1-1/8 inches long and the brass flanges were 5/16-inches long.

Two heaters, a 99 ohm calorimeter heater and a 1.5 ohm trickle heater, were held in the heater well (1-D) in each container lid. The calorimeter heaters were made from noninductively wound 38 B and S gauge manganin wire, and the trickle

heaters were made from 30 B and S gauge manganin wire. The wire was wound around thin mica supports and the heaters were annealed at 140°C. for 48 hours prior to insertion into the heater wells. The remaining volume in the heater wells was filled with melted paraffin wax to improve heat conduction from the heaters.

Leads for both types of heaters were made from 30 B and S gauge copper wire. Potential leads of 36 B and S gauge copper wire were connected to the midpoint of the calorimeter heater leads. The leads from each heater assembly were passed to the external circuits via six-conductor shielded cable to which they were connected at a teflon junction block (1-K) attached to the underside of the submarine lid. The calorimeter heater and circuit is shown in Figure 2 and the trickle heater circuit in Figure 3. The calorimeter heater circuit is regulated through use of two Leeds and Northrup 12-position silver contact rotary switches (2-C, 2-D). Switch 2-C was wired so that the potential drop across either heater, across both heaters in series, across the standard resistor (2-E), or across a dummy heater (2-F) could be measured. Switch 2-D was wired so that current could be passed through either heater, through both heaters in series, or through a dummy heater (2-F). When switch 2-D allowed current to pass through a heater an electronic timer (2-G) was engaged.

The current sources for the calorimeter heaters were low discharge lead storage batteries. The following arrangements

were used: a 2-volt battery (2-V$_1$); two 6-volt batteries in parallel (2-V$_2$, 2-V$_3$); and four six-volt batteries (2-V$_1$, 2-V$_2$, 2-V$_3$, 2-V$_4$) arranged to give a 12-volt working potential. An A.C. source was used for rapidly bringing the calorimeter containers to operating temperature and was disconnected at all other times.

The liquid in the calorimeter containers was mixed with stainless steel stirrers (1-E). Two semicircular vanes were set at a 60° angle to each other and were riveted to the end of a 4 inch long 1/8-inch stainless steel rod. The rod screwed into an inch long nylon spacer which in turn screwed into a 12-inch long 1/4-inch stainless steel stirrer shaft. Each stirrer shaft passed through two New Departure number 77R4A sealed bearings; one mounted immediately above the submarine lid and the other mounted 3 inches above the water bath lid. A bakelite pulley was attached to the top of each stirrer shaft and the stirrers were driven at 325 r.p.m. by a 325 r.p.m. synchronous motor using an O-ring as a drive belt.

The sample holders were thin-walled annealed pyrex bulbs. The bulbs were approximately spherical in shape and ranged in size from 4 milliliters to 20 milliliters. The sample bulbs were held by their necks in a stainless steel support. Two bulbs smaller than 8 milliliters or one bulb larger than 8 milliliters could be accommodated by the support. Lack of room in the calorimeter containers limited the maximum bulb size to 20 milliliters.

The sample holder rods (1-F) extended above the bath lid so that the samples could be manipulated when the calorimeter was assembled. Each sample holder rod was made up of three pieces: an upper 8-inch length of 1/4-inch stainless steel rod, a lower 6-inch length of 1/4-inch tantalum rod, and a 1-inch length of 1/4-inch stainless steel tube which held the other two pieces together. The sample holder support screwed onto the end of the tantalum rod.

The sample breakers were pointed 1/4-inch stainless steel rods cemented to the floors of the calorimeter containers. A sample bulb was broken by lowering it against a breaker. When two sample bulbs were supported in one container either bulb could be positioned over the breaker by rotating the sample holder rod.

The water bath was adiabatically controlled at the mean temperature of the two calorimeter containers. The temperature difference was sensed with two 5-junction copper-constantan thermopiles (2-J, 2-J'). One end of a control thermopile was held by a copper tube (1-L) which extended into the water bath through the submarine lid. The other end of a control thermopile was held by the 1/4-inch tantalum tube welded into the container lid (1-G). Each copper tube and tantalum well was filled with melted paraffin wax.

The control thermopiles were constructed from 36 B and S gauge copper wire and 30 B and S gauge constantan wire and had 36 B and S gauge copper leads. The leads from the two

thermopiles were connected to a teflon junction block attached to the bottom of the submarine lid. A shielded four-conductor cable carried the control thermopile signals from the junction block to a Leeds and Northrup 12-position silver contact rotary switch (2-K). This switch was wired so that it could pass either thermopile signal, the two signals in series, or the two signals in opposition. In operation the two thermopiles were switched in series to obtain the maximum signal. From this switch the signal was passed through an Aryton shunt (2-M) to the automatic bath controller (2-L). The bath controller (which was built by the Ames Laboratory Electronics Shop) amplified the signal approximately 10^6 times and fed the output to a Thyratron relay switch which operated the 500-watt Calrod bath control heater. The bath heater was connected in series with a Variac (2-P) to control the heating rate.

Optimum balance between the heating rate and the cooling water flow rate gave alternate heating and cooling periods of 15 to 30 seconds each with a temperature oscillation in the water bath of $\pm 0.0005^{\circ}C$. The temperature of the water bath rose approximately $0.001^{\circ}C.$ per hour following the temperature rise of the calorimeter containers due to heat generated by the calorimeter stirrers. The water bath temperature was read to a hundredth of a degree from a mercury thermometer. When more accuracy was needed the temperature was determined to a thousandth of a degree with a platinum resistance thermometer, calibrated by the National Bureau of Standards, in conjunction

with a Leeds and Northrup Model G-2 Mueller Temperature Bridge.

The temperature difference between the calorimeter containers was sensed with the main thermopile (1-J). The main thermopile consisted of two 30-junction thermopiles (3-U, 3-U') made from 36 B and S gauge copper wire and 30 B and S gauge constantan wire with 36 B and S gauge copper leads. The thermopiles were constructed over thin 7 centimeter by 12 centimeter mica forms and were shielded by a copper casing which fit snugly into the thermopile wells in the calorimeter containers.

The thermopile leads were connected to a teflon junction block fastened under the submarine lid. The thermopile signals were carried through four-conductor shielded cable to a Leeds and Northrup 12-position rotary silver contact switch (3-V) wired so that the signals could be passed individually, in series, or in opposition. From the rotary switch the signal was passed to a Liston Becker Model 14 breaker-type D.C. amplifier (3-W). The output from the amplifier was passed through a Liston Becker filter circuit (3-X) to reduce the noise level and finally the signal was displayed on a 60 millivolt Brown recording potentiometer (3-Y). A Stabiline type IE-5101 voltage regulator (3-Z) served as a constant power supply for the amplifier and recorder.

V. SOLUTION PREPARATION

Rare-earth oxides were obtained from the rare-earth separation group of the Ames Laboratory. Purity of the oxides was established by emission spectrography to be better than 99.9 per cent. The major impurities in any rare-earth oxide were iron, calcium, and adjacent rare-earths.

Rare-earth chloride stock solution was prepared by dissolving an excess of the rare-earth oxide in C. P. grade hydrochloric acid and filtering the solution through sintered glass to remove the undissolved oxide. This resulted in a colloidal rare-earth chloride solution basic with respect to the equilibrium pH of the hydrolysis equilibrium as represented by equation 5.1.

$$R^{3+} + H_2O = ROH^{2+} + H^+ \tag{5.1}$$

Aliquots of the stock solution were titrated with dilute hydrochloric acid using a glass electrode versus a calomel reference electrode. The equivalence pH of the solution was determined from a plot of pH versus titrant volume. The solution was adjusted to the equivalence pH and was heated to 100°C. to facilitate the reaction of the acid with the colloidal species. If the heating caused a rise in the room temperature pH, the stock solution was readjusted to its equivalence pH and heated again. These steps were repeated until the pH no longer changed with heating.

Analyses were carried out to determine both the rare-earth and chloride concentrations of the stock solutions. Three methods were used for rare-earth analysis and one method for chloride analysis.

(1.)   Oxide analysis. Rare-earth chloride solution was weighed into ceramic crucibles, the rare-earth was precipitated with a 20 per cent excess of twice recrystallized oxalic acid, and the precipitate was dried under IR lamps and fired to the oxide at 900°C. in a muffle furnace. The samples were weighed as rare-earth oxide R_2O_3.

(2.)   Sulfate analysis. Rare-earth chloride solution was weighed into ceramic crucibles, precipitated with an excess of six normal sulfuric acid, and the excess acid was removed as sulfur trioxide by heating with a Meeker burner. The samples were ignited in a muffle furnace at 500°C. and were weighed as rare-earth sulfate $R_2(SO_4)_3$.

(3.)   EDTA analysis. Rare-earth chloride solution was weighed into a flask and the rare-earth was titrated with two-hundredth molal disodium dihydrogen ethylene diammine tetraacetate (EDTA) from a weight burette. Methyl orange was used as the endpoint indicator, the titrate was buffered to pH 5, and pyridine was added to sharpen the endpoint. The EDTA solution was standardized versus a zinc chloride solution

which had been prepared by weight from electrolyti-
cally prepared zinc metal.

(4.) Chloride analysis. Chloride analyses were carried
out by a potentiometric method using a Sargent Model
D Recording Titrator. The electrode system con-
sisted of a silver chloride indicator electrode and
a sleeve-type reference electrode with an ammonium
nitrate bridge to the inner calomel electrode. Rare-
earth chloride was weighed into a flask and the
chloride was titrated with one-tenth molal silver
nitrate solution from a weight burette. The course
of the reaction was followed on the recording
titrator. The silver nitrate solution was standard-
ized versus a potassium chloride solution which had
been prepared by weight from recrystallized potassi-
um chloride.

All the analyses were performed in triplicate, usually
with a precision of ± 0.05 per cent. Agreement between the
different methods was ± 0.1 per cent or better. The oxide
analyses usually gave slightly higher results than any of the
other three methods.

A series of dilutions was prepared from weighed additions
of the rare-earth chloride stock solutions and conductivity
water. The conductivity water had a specific conductance of
less than 1×10^{-6} mho per centimeter. It was made by dis-
tilling tap distilled water from an alkaline potassium

permanganate solution in a Barnstead Conductivity Still. The
dilutions ranged in concentration from one-hundredth molal to
saturation in approximate steps of one-tenth $m^{1/2}$ units.

Saturated rare-earth chloride solution was prepared by
desiccating a quantity of stock solution over magnesium per-
chlorate at room temperature until crystals appeared. The so-
lution and crystals were placed in a flask mounted on a shaker
arm in a water bath controlled at $25.00 \pm 0.01^{\circ}C.$ and allowed
to equilibrate for at least two weeks. Saturated solution was
pipetted from the flask after the crystals had settled to the
bottom.

The concentrations of saturated $NdCl_3$, $SmCl_3$, $GdCl_3$, $DyCl_3$,
and $ErCl_3$ solutions were taken from the data of Saeger (45),
and the concentrations of saturated $EuCl_3$, $TmCl_3$, and $LuCl_3$ so-
lutions were taken from the data of Spedding and Weber[1].

Wet crystals grown in the above manner were filtered from
the solution, dried over magnesium perchlorate, ground, and
finally dried over calcium chloride. Weighed samples of the
crystals were titrated with EDTA to determine when the excess
water was removed. The crystals were removed from the desiccant
when an EDTA analysis indicated the rare-earth composition to
be within 0.1 per cent of its theoretical composition. The

---

[1]Spedding, F. H. and Weber, H. O., Ames Laboratory of the
A.E.C., Ames, Iowa. Activity coefficients of some rare-earth
chloride solutions. Private communication. 1966.

crystals were never dehydrated below their theoretical water composition. Crystals of $LaCl_3$ and $PrCl_3$ hydrates grown from saturated solution at 25°C. have a composition of seven waters of hydration per rare-earth. Crystals of $NdCl_3$, $SmCl_3$, $EuCl_3$, $GdCl_3$, $DyCl_3$, $ErCl_3$, $TmCl_3$, $YbCl_3$, and $LuCl_3$ hydrates have a composition of six waters of hydration per rare-earth.

All weights determined in the course of an analysis or dilution were corrected to vacuum.

VI. EXPERIMENTAL PROCEDURE

The following procedure was used for all heat of dilution and heat of solution experiments.

The samples were prepared on the day prior to a run. Samples of rare-earth chloride solution were introduced into the sample bulbs with either a stainless steel tipped syringe or a glass pipet. The sample bulbs were capped with teflon plugs while they were weighed. After the final weighings the sample bulbs were sealed shut with Apiezon wax. This was accomplished by heating the end of a bulb neck in a flame and introducing a small amount of melted wax into the neck. There was no danger of heating the samples during this step since the bulbs were hand held lower down on the necks. Considerable care had to be exercised while filling and handling the sample bulbs to keep sample solution out of the bulb necks. Solution lodged in a bulb neck and separated from the rest of the sample solution would not undergo dilution when the bulb was broken. Such cases were easily spotted and the results for these samples were rejected.

Samples of the hydrated crystals were introduced into the sample bulbs with only a brief exposure to the atmosphere. A small glass tube with one end drawn out was filled with the crystals and capped. The drawn-out end of the tube was inserted into a sample bulb neck and the salt was tapped into the bulb. The sample bulbs were weighed and sealed in the same

manner as when they contained solution samples.

On the day of a run conductivity water was weighed into the calorimeter containers, subject to the criterion that the total liquid weight equal 900 grams, and the apparatus was assembled. Room temperature was always below 25°C. and consequently the following steps always involved heating the water bath and calorimeter containers to the operating temperature. Immediately after assembly either the containers or the water bath, whichever was the cooler, was heated to within 0.001°C. of the other and the automatic adiabatic water bath temperature control was initiated. The temperature differential between the calorimeter containers was then reduced to less than 0.0001°C. Finally, the temperature of the entire assembly was raised to 24.95°C. This was accomplished by first heating the water bath to that temperature using the auxiliary bath heater and then by heating the calorimeter containers in series with the A.C. current source until the temperature controller indicated that the bath temperature had been reached. Final adjustments were made in the heating and cooling rates and the system was allowed to stand for three to four hours. This was usually sufficient time to establish near-equilibrium conditions throughout the system.

The first heat was not carried out until a constant-slope thermopile e.m.f. trace had been recorded for at least 45 minutes. Unless an adjustment was made in the system the foreslope of any particular heat was the afterslope of the

previous heat. The first heat to be carried out was the determination of the heat capacity ratio. The 12-volt current source was used through the two calorimeter heaters in series to add 30 calories to each container. A difference in heat capacity between the two containers caused an unequal temperature rise and showed up as a deflection in the recorder trace. The heat capacity ratio, which was used as a multiplicative correction to chemical heats, was calculated from this deflection.

The theory of operation of a twin calorimeter involves the balancing of chemical heat in one container with electrical heat in the other. It is thus imperative that a given quantity of heat causes an equal temperature rise in each calorimeter container. If this is not the case the difference must be accounted for by a correction. For all but a very few experiments the heat capacity ratio was within 0.05 per cent of unity.

Two calibration heats were carried out after the heat capacity determination. These experiments determined the sensitivity of the calorimeter in terms of calories per millimeter recorder chart deflection. Most of the experiments were carried out at a setting on the Liston Becker amplifier of gain 18, which corresponded to a sensitivity of approximately 4.2×10^{-4} calories per millimeter chart deflection. On gain

1S a full chart deflection corresponded to a temperature change of about 0.0001°C. or to about 0.1 calories of heat. The 2-volt current source with resistance from a variable resistance box switched in series with the heater was used to generate 0.04 to 0.05 calories in a typical calibration heat. On an amplifier setting of gain 19, which was used only in experiments where less than 2 calories of chemical heat were evolved, the calorimeter had a sensitivity of about 2.9×10^{-4} calories per millimeter chart deflection.

The sample breaks were carried out last. A dilution or solution experiment was carried out by switching the 6-volt current source into the calorimeter heater in one container, reading the potential drop across the standard resistor and, halfway through the heating period, breaking the sample bulb in the other container. The auxiliary water bath heater was regulated by hand during the heating period to maintain adiabatic conditions. The correct electrical heat was usually added to within two per cent to balance the chemical heat. Within ten to fifteen minutes of the break a smaller heat, with the 2-volt current source, could be estimated closely enough to bring the recorder trace to within a few inches of its original position.

Sample bulbs were broken halfway through the heating periods to keep the maximum temperature difference between the calorimeter containers as small as possible. Since electrical heat is evolved at a linear rate and chemical heat at an exponential rate, each container was hotter than the other for

about one half the heating period. This served to minimize the
net heat leaked between the containers. The heating periods for
dilution samples were rarely longer than one and one half mi-
nutes.

For at least 20 minutes prior to any heating period
current from the source to be used was passed through a 99 ohm
dummy heater. This stabilized the batteries and helped hold
potential drifts during the heating periods to a minimum.

The electrical heat generated in a calorimeter container
was calculated according to equation 6.1, where R_H is the re-
sistance of the heater, R_S the resistance of the standard
resistor, E_S the potential drop across the standard resistor, t
the time, and 4.184 the joulecalorie conversion constant.

$$q_{el.} = \frac{R_H(E_S)^2 t}{4.184(R_S)^2} \tag{6.1}$$

The heat evolved from the dilution of the sample was
calculated by making the following four corrections to the
electrical heat.

Water vapor equilibrates at a lower pressure above a rare-
earth chloride sample solution than above the very dilute so-
lution resulting from its dilution. Thus when a sample is
diluted water will evaporate into the free volume of the sample
bulb. This evaporation exerts a cooling effect which cancells
part of the dilution heat. The relative size of this effect
increases with the solute concentration (as the equilibrium

vapor pressure over the solution decreases). The evaporation
correction was negligible at concentrations lower than 1 molal
but amounted to as much as 0.05 calories at 4 molal. The
correction was estimated according to the following equations,

$$q_{evap.} = \frac{273}{298} \frac{P}{760} \frac{V}{22400} \ 10514 \text{ calories} \qquad (6.2)$$

$$q_{evap.} = 0.000566 V \Delta P \text{ calories} \qquad (6.3)$$

where V is the volume in milliliters of the empty fraction of
the sample bulb, ΔP is the difference in millimeters mercury
between the vapor pressure over the sample solution and over
pure water, and 10514 is the latent heat of vaporization of
water according to Rossini (44).

A small amount of heat is evolved when the sample bulbs
are broken. This heat effect was usually small enough to be
within the limits of accuracy of the measurements, but since
the correction had been determined it was applied to all experi-
ments. The glass sample bulbs were hand blown and did not have
uniform wall thicknesses. If the bulb walls are sufficiently
thin the bulbs will elastically deform before they break. The
bulbs were pressed against a postal scale platform and sepa-
rated into groups according to the scale reading observed when
they began to deform. The heats of breaking of bulbs from each
group were measured and the results are given by equation 6.4
where S is the magnitude of the scale reading in ounces.

$$q_{open} = 0.00060 \text{ S calories} \qquad (6.4)$$

There is an estimated 50 per cent uncertainty in the heat of
opening values calculated from equation 6.4. The glass bulbs
were used as sample bulbs only if they began to deform at
readings of 4 ounces or less.

The electrical heat was seldom estimated closely enough to
exactly balance a chemical heat. The correction for the amount
by which the system was overheated or underheated was based on
the distance of separation of the recorder trace after the break
from the trace before the break. These traces usually had
slightly different slopes. The established procedure of previ-
ous investigators was to measure the distance between the traces
at the point of the break and at the point where the afterslope
became linear, and to base the chart correction on the average
of these two distances. This procedure was modified slightly
in this research by basing the chart correction only on the
distance of separation of the traces at the point of the break.
This change was justified on the basis of evidence which indi-
cated that the slope change took place at or shortly after the
time of the break. In the heat of opening experiments, where
the sample bulbs were filled with water and where only very
small heats were evolved, the trace would become linear with a
new slope within a few minutes of the break (as rapidly as the
calorimeter could respond to the heat effect). All slope
changes which occurred when a sample bulb was broken were in a
direction to indicate a small continuous heat effect in the
container in which the break had been made. It was postulated

that these slope changes were due in large part to heat gener-
ated by turbulent flow of the solution past the jagged sample
bulb edges. The chart correction was calculated by multiplying
the distance of separation of the traces by the sensitivity
determined from the calibration experiments. The slope changes
were usually quite small and chart corrections calculated by
either method only rarely accounted for a difference greater
than 0.1 per cent in the final result.

The reason for the heat capacity correction has already
been discussed. The heat capacity correction is applied in the
following manner. Assume that a chemical heat took place in
container I and was balanced by electrical heat in container II.
The corrected heat evolved in container I is given by equation
6.4, where C_I/C_{II} is the ratio of the heat capacity of container
I plus contents to that of container II plus contents.

$$q_I = \frac{C_I}{C_{II}} \, q_{II} \qquad (6.4)$$

This correction was applied only to the sum of the electrical
heat plus the chart correction. Heat capacity ratios determined
at the end of any experiment (after all the samples were
diluted) were identical with those determined at the beginning.

The evolved chemical heat due to the dilution or solution
of a sample is given by equation 6.5,

$$q_{dil.} = (q_{el.} \pm q_{chart})C' + q_{evap.} - q_{open} \qquad (6.5)$$

where the various corrective quantities are identified by their subscripts, and C' refers to the heat capacity ratio.

The enthalpy of neutralization of hydrochloric acid was measured as a test of the calorimeter and the experimental technique. There are as yet no primary standards for aqueous solution calorimetry. The neutralization of hydrochloric acid was chosen as a test reaction because it has been well characterized and because it could be carried out in almost exactly the same manner as a dilution experiment.

The reaction is given by equations 6.6 and 6.7, where ΔH_N is the enthalpy of neutralization of the acid and $\Delta H_N{}^0$ is the enthalpy of neutralization of the acid at infinite dilution.

$$NaOH(m) + HCl(m) = NaCl(m) + H_2O \qquad (6.6)$$
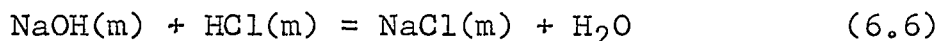
$$\Delta H_N = \Delta H_N{}^0 + \emptyset_L(NaCl, m) - \emptyset_L(HCl, m) -$$
$$\emptyset_L(NaOH, m) \qquad (6.7)$$

Values of $-\Delta H_N{}^0$, the enthalpy of ionization of water, have recently been determined by Vanderzee and Swanson (57) who reported 13336 ± 18 calories per mole, and by Hale, Izatt, and Christensen (25) who also reported 13336 ± 18 calories per mole. Both investigators give brief discussions of some of the older reported values for $-\Delta H_N{}^0$ and offer explanations for the apparent discrepancies.

The hydrochloric acid was made up to a concentration of 0.15857 molal by weight dilution from constant boiling hydro-

chloric acid according to the results of Foulk and Hollingsworth
(9). Standardization versus potassium hydrogen phthalate indi-
cated an acid concentration of 0.15846 molal. Carbonate free
concentrated sodium hydroxide solution was prepared by a
standard method (58a).

The acid was exposed to no other metals besides tantalum.
A glass pipet was used to introduce the acid into the sample
bulbs. The stainless steel parts in the calorimeter containers
were replaced with similar tantalum pieces.

Conductivity water was weighed into the calorimeter con-
tainers and, immediately prior to assembly of the apparatus,
enough concentrated sodium hydroxide solution was pipeted into
each container to give a solution approximately 0.003 molal in
sodium hydroxide. This gave a 3-fold excess of base over acid
in each calorimeter container. The dilute sodium hydroxide so-
lutions had insufficient time to saturate with carbon dioxide
before they were closed off from the air.

The results of a neutralization experiment can be serious-
ly affected by the thermal effects of shifts in the carbonate-
bicarbonate-carbon dioxide equilibrium. This problem was
circumvented in these experiments by using an excess of base in
a solution deficient in carbon dioxide.

Since the hydrochloric acid was the limiting reactant it
was necessary to know the concentration of the sodium hydroxide
solution only to within about 10 per cent.

According to Harned (26) the thermodynamic properties of

each electrolyte in a mixture are a function of the total ionic strength of the solution. From the work of Young, Wu, and Krawetz (66) and Wood and Smith (61) the heat of mixing of sodium hydroxide and sodium chloride can be assumed to be negligible at low ionic strengths.

At the low concentrations used in these experiments the apparent molal heat contents of sodium hydroxide and sodium chloride are indistinguishable (44, 57). Since the two salts appear in equimolar amounts in equation 6.6 their contribution to the enthalpy of neutralization will therefore cancel, and equation 6.7 can be reduced to the following expression.

$$\Delta H_N^o = \Delta H_N + \phi_L(HCl, m) \tag{6.8}$$

A total of four samples were run; two in each calorimeter container. The average enthalpy of reaction was $\Delta H_N = -13496$ calories per mole, with a mean deviation of 5 calories per mole. At a concentration of 0.1585 molal, hydrochloric acid has an apparent molal heat content of 165 calories per mole (57). Combining this with the enthalpy of reaction gives, according to equation 6.8, $\Delta H_N^o = -13331 \pm 5$ calories per mole. This result is in excellent agreement with the previously cited values and is taken to be a confirmation of the validity of the experimental technique. The uncertainty in the final result is a measure only of the precision of these particular experiments. An uncertainty of 0.1 per cent in the hydrochloric acid concentration would lead to a more reasonable result of

$\Delta H_N{}^O$ = -13331 $\pm$ 18 calories per mole for the enthalpy of neutralization of hydrochloric acid at 25°C.

All weights taken in any part of this procedure were corrected to vacuum and the experiments were carried out at 25.00 $\pm$ 0.01^{O}C.

VII. CALCULATIONS AND RESULTS

When a rare-earth chloride solution of malality m_1 containing n_2 moles of solute is diluted into pure water to a final molality of m_2, q_{dil} calories of heat are evolved and the enthalpy of dilution per mole of solute is given by equation 7.1.

$$\Delta H_{1,2} = \frac{q_{dil}}{n_2} \qquad (7.1)$$

The subscript on H implies that the dilution took place from a solution of molality m_1 to a solution of molality m_2. This quantity was referred to as ΔH_D in the section on thermodynamics. When a second sample of rare-earth chloride solution of molality m_1 containing n_2' moles of solute is diluted into the solution resulting from the first dilution, q'_{dil} calories of heat are evolved, the final molality is m_3, and the enthalpy of dilution per mole of solute is given by equation 7.2.

$$\Delta H_{1,3} = \frac{q_{dil} + q'_{dil}}{n_2 + n_2'} \qquad (7.2)$$

These last two equations can be combined to give the enthalpy of dilution over the concentration range m_3 to m_2.

$$\Delta H_{3,2} = \Delta H_{1,2} - \Delta H_{1,3} \qquad (7.3)$$

The quantities $\Delta H_{1,2}$ and $\Delta H_{1,3}$ are called long chords of dilution and $\Delta H_{3,2}$ is called a short chord of dilution.

The values of ϕ_L at low concentrations can be determined

from the short chord data. A theorem of mathematical analysis states that for a polynomial g(x), if the difference in g(x) at the endpoints of an interval is divided by the length of the interval, the quotient will represent a polynomial reduced by an order of one from the original polynomial g(x). An alternative statement is that this quotient represents the mean value of the derivative of g(x) over the interval as shown by equation 7.4.

$$\frac{d}{dx} g(x) = \frac{g(x_2) - g(x_1)}{x_2 - x_1} \qquad (7.4)$$

Young and coworkers (63, 65) first applied this idea to heat of dilution studies. If the slope of the enthalpy of dilution curve is labelled P_i, the average value of P_i over the concentration interval m_3 to m_2 is represented by an expression analogous to equation 7.4.

$$\overline{P}_i = \frac{\emptyset_L(m_3) - \emptyset_L(m_2)}{(m_3)^{1/2} - (m_2)^{1/2}} = \frac{\Delta H_{3,2}}{(m_3)^{1/2} - (m_2)^{1/2}} \qquad (7.5)$$

A series of dilutions gave, for each rare-earth chloride, a set of short chord dilutions over concentration intervals whose midpoints ranged between $m^{1/2} = 0.03$ and $m^{1/2} = 0.08$. Analytical expressions for $\overline{P}_i$ versus $m^{1/2}$ were obtained graphically from plots of the $\overline{P}_i$ points versus the interval midpoints. Over the concentration range investigated in this research the $\overline{P}_i$ curves proved to be linear with respect to $m^{1/2}$ within experimental error and were extrapolated as linear functions to

zero concentration.

$$\overline{P}_i = A - 2Bm^{1/2} \qquad\qquad (7.6)$$

The Debye-Hückel limiting law predicts the limiting slope of
the $\emptyset_L$ curves for 3-1 electrolytes at 25°C. to be 6925. All
the $\overline{P}_i$ curves determined in this research extrapolated to with-
5 per cent of that value at zero concentration. Therefore the
intercept value of the $\overline{P}_i$ curves was taken to be 6925 to help
reduce the uncertainty in the limiting $\emptyset_L$ equations.

Equation 7.6 was integrated to give an expression for $\emptyset_L$
in the limiting law region.

$$\emptyset_L \ (m) = Am^{1/2} - Bm \qquad (0 \quad m^{1/2} \quad 0.08) \quad (7.7)$$

The A term in equations 7.6 and 7.7 is the limiting slope of
the enthalpy of dilution curves at zero concentration.

Previous investigators (2, 4, 5, 37) carried out measure-
ments on large quantities of dilute solutions to obtain short
chord data over the concentration range $m^{1/2} = 0.01$ to $m^{1/2} =$
0.03. These dilute solutions evolved very small quantities of
heat and due to the experimental error the relative precision
of this data was quite low. The low concentration $\overline{P}_i$ data was
thus scattered and proved to be of relatively little help,
compared to data from higher concentration regions, in es-
tablishing an experimental limitng slope. In the present re-
search all the short chord data was obtained by diluting so-
lutions of concentrations higher than $m^{1/2} = 0.50$ in order to

get dilution heats large enough to be measured with a minimum of relative error.

After establishing an expression for $\emptyset_L$ for a rare-earth chloride through the limiting regions, the $\Delta H_{1,3}$ values were recalculated from the following equation.

$$\Delta H_{1,3} = \frac{q' + n_2 \Delta H_{3,2}}{n_2'} \tag{7.8}$$

The values used for $\Delta H_{3,2}$ in the above equation were calculated from the expression for $\emptyset_L$ in the limiting law region, equation 7.7. In this way no individual experimental error in a $\Delta H_{1,2}$ value was carried over into the corresponding $\Delta H_{1,3}$ value.

All the final concentrations from the dilution experiments fell within the concentration range for which equation 7.7 is valid, and the $\emptyset_L$ values for the original solution were calculated according to equation 3.27.

The $\emptyset_L$ curves are split into three segments for ease of representation.

(1.) The limiting law region, $0 < m^{1/2} < 0.08$. $\emptyset_L$ is represented over this region by a second order least square polynomial according to equation 7.7.

(2.) The dilute region, $0 < m^{1/2} < 0.50$. $\emptyset_L$ is represented analytically by a least square polynomial of the form of equation 7.9.

$$\emptyset_L(m) = bm^{1/2} + cm + dm^{3/2} + em^2 \tag{7.9}$$

(3.) The concentrated region, $m^{1/2} > 0.50$. $\emptyset_L$ is represented analytically by a least square polynomial of the form of equation 7.10.

$$\emptyset_L(m) = a' + b'm^{1/2} + c'm + d'm^{3/2} + e'm^2 \quad (7.10)$$

The parameters in equation 7.9 and 7.10 were generated from a standard double precision orthogonal polynomial least squares program run on an IBM 360 computer. All other equations expressing thermodynamic quantities as high order least squares polynomials were generated in the same manner.

The experimental data for the heats of dilution of the eight rare-earth chlorides determined in this research are presented in Tables 1-8. The first column in these tables lists the concentration of the solution; the second column gives the number of moles of rare-earth in each sample; the third column gives the square root of the final molality after each dilution; the fourth column gives the heat of dilution of each sample, corrected according to equation 6.6; the fifth column gives the values of $\overline{P}_i$; and the sixth column gives the experimental $\emptyset_L$ value of the solution. An asterik after a number in the second column indicates this sample was broken into the solution resulting from the dilution of the immediately preceding sample. Occasionally the experimental value from a dilution was rejected. Results were rejected only when it was clear that the reasons for rejection were valid: for example, incomplete mixing of the sample, electronic failure, or operator

error.

All other terms used in the calculation of the $\emptyset_L$ or $\overline{P}_i$ values listed in Tables 1-8 can be calculated from the data listed in these tables.

Parameters for the $\overline{P}_i$ expressions were determined graphically according to equation 7.6 and are given in Table 9. The Debye-Huckel limiting slope was assumed as the intercept value for all the $\overline{P}_i$ curves. A plot of the $\overline{P}_i$ data for $SmCl_3$ is shown in Figure 4.

The average values at each concentration of the $\emptyset_L$ data were represented as least square polynomials according to equations 7.9 and 7.10. The parameters for these polynomials are listed in Tables 10 and 11.

Values for $\overline{L}_1$ and $\overline{L}_2$ were calculated from the $\emptyset_L$ polynomials according to equations 3.21 and 3.22 and are listed at selected molalities in Tables 12-19. Values of $\overline{L}_1$ and $\overline{L}_2$ are represented as least square polynomials according to equations 7.11 and 7.12.

$$\overline{L}_1(m) = Dm^{3/2} + Em^2 + Fm^{5/2} + Gm^3 \qquad (7.11)$$

$$\overline{L}_2(m) = A' + B'm^{1/2} + C'm + D'm^{3/2} + E'm^2 \quad (7.12)$$

The parameters for equations 7.11 and 7.12 over the low concentration range ($m^{1/2} = 0$ to $m^{1/2} = 0.5$) are given in Tables 20 and 21, and the parameters for these equations over the rest of the concentration range are given in Tables 22 and

23.

Partial molal excess entropies were calculated according to equations 7.13 and 7.14.

$$T(\bar{S}_1 - \bar{S}_1{}^\circ) = \bar{L}_1 - RT\ln\frac{a_1}{N_1} \qquad (7.13)$$

$$T(\bar{S}_2 - \bar{S}_2{}^\circ) = \bar{L}_2 - vRT\ln f_\pm \qquad (7.14)$$

Values for a_1/N_1, the activity coefficients of the solvent, and $f_\pm$, the activity coefficients of the solute, were taken from the data of Saeger (45), Petheram (39), and Spedding and Weber[1]. Values of $T(\bar{S}_1 - \bar{S}_1{}^\circ)$ and $T(\bar{S}_2 - \bar{S}_2{}^\circ)$ at selected molalities are listed in Tables 12-19.

Figure 5 shows a plot of $\emptyset_L$ versus $m^{1/2}$ for the eight rare-earth chlorides measured in this research and the five rare-earth chlorides measured by DeKock (4). Figure 6 shows a plot of $\emptyset_L$ for the rare-earth chlorides versus rare-earth at three values of $m^{1/2}$. Figures 7 and 8 show, respectively, plots of $\bar{L}_1$ and $\bar{L}_2$ versus molality for $SmCl_3$. Figure 9 shows a plot of values of $\bar{L}_2$ for the rare-earth chlorides versus rare-earth at three molalities. Figures 10 and 11 show, respectively, plots of $T(\bar{S}_1 - \bar{S}_1{}^\circ)$ and $T(\bar{S}_2 - \bar{S}_2{}^\circ)$ versus molality for $SmCl_3$, and Figure 12 shows a plot of values of $T(\bar{S}_2 - \bar{S}_2{}^\circ)$ for the rare-earth chlorides at three molalities.

---

[1]Spedding, F. H. and Weber, H. O., Ames Laboratory of the A.E.C., Ames, Iowa. Activity coefficients of some rare-earth chloride solutions. Private communication. 1966.

Figures 5, 6, 9, and 12 include results determined by DeKock
(4).

When n_2 moles of hydrated rare-earth chloride crystals are
dissolved in water to give a solution of molality m_2, $q_{sol.}$
calories of heat are evolved and the enthalpy of solution of
the crystal to molality m_2 is given by equation 7.15.

$$\Delta H_s (m_2) = \frac{q_{sol.}}{n_2} \qquad (7.15)$$

When n_2' moles of hydrated rare-earth chloride crystals are
dissolved in the above solution to give a solution of molality
m_3, $q_{sol.}'$ calories of heat are evolved and the enthalpy of
solution of the crystals to molality m_3 is given by equation
7.16.

$$\Delta H_s (m_3) = \frac{q'_{sol.} + n_2 \Delta H_{3,2}}{n_2'} \qquad (7.16)$$

The molar heat content of the crystals (the heat of solution to
infinite dilution) is calculated according to equation 3.32.

The experimental data determined in this research for the
heats of solution of eleven hydrated rare-earth chlorides are
listed in Table 24. The first column in Table 24 identifies
the hydrate; the second column gives the number of moles of
rare-earth in each hydrate sample; the third column gives the
square root of the molality of the final solution; the fourth
column gives the heat of solution of the hydrate crystal;
and the fifth column gives the relative molar heat content of

the crystal. Figure 13 shows a plot of the molar heat contents of the rare-earth chloride hydrates. The results of DeKock (4) for $TbCl_3 \cdot 6H_2O$ and $HoCl_3 \cdot 6H_2O$ are included.

The heat of neutralization experiments establish the uncertainty in the absolute accuracy of the calorimeter to be less than $\pm$ 0.15 per cent of the measured values when these values are on the order of 4 to 7 calories.

Whenever the heats of dilution of two or more samples of a given solution were measured the per cent deviation of each experimental value from the average value was determined. A total of 430 results were obtained from 148 experiments where two or more similar samples were measured. The experimental differences from the average values of these results could be accounted for in 81 per cent of the cases by absolute errors of 0.006 calories or by relative errors of 0.1 per cent. The differences of the experimental values from the mean values could be accounted for in 94 per cent of the cases by absolute errors of 0.009 calories or by relative errors of 0.15 per cent. Most of the differences which fell outside these limits were obtained from measurements on solutions in the concentration range $m^{1/2} = 0.1$ to $m^{1/2} = 0.4$ where the dilution heats were relatively small. An estimate of the experimental error must also include an uncertainty of 0.1 per cent in the solution concentrations. This gives a total relative uncertainty of $\pm$ 0.25 per cent in the $\emptyset_L$ values due to experimental errors.

The Debye-Hückel limiting law value for 3-1 electrolytes

Table 1. Observed heats of dilution of aqueous neodymium chloride solutions at 25°C.

m_1	$n_2 \times 10^4$	$m_f^{1/2} \times 10^2$	$-q_{dil.}$ cal.	$\bar{P}_i$	$\emptyset_L(m_1)$ cal./mole
0.05293	10.912	3.4831	0.798		954
0.09959	17.584	4.4159	1.542		1153
0.1726	24.884	5.254	2.581		1359
	29.623	5.740	3.003		1361
0.2532	38.770	6.568	4.406		1525
0.3597	45.423	7.100	5.823		1696
	48.263	.7.329	6.148		1699
0.4927	47.006	7.223	6.873		1882
	42.368	6.866	6.268		1882
0.6407	30.163	5.804	5.185		2070
	33.954*	8.438	5.392	4870	2063
	35.394	6.377	5.990		2072
	35.663*	8.896	5.575	4860	2056
0.8008	29.646	5.758	5.669		2260
1.006	25.770	5.355	5.591		2497
	26.114*	7.588	5.380	4920	2497
	26.067	5.394	5.644		2494
	26.413*	7.643	5.432	4880	2496
1.221	20.308	4.752	5.002		2757
	20.709*	6.747	4.888	5150	2757
	20.247	4.751	4.976		2752
	20.298*	6.717	4.784	5130	2753
1.455	18.692	4.557	5.170		3050
	18.750*	6.446	5.003	5220	3051
	18.001	4.478	4.984		3048
	18.246*	6.350	4.871	5290	3048

*In this table, and all succeeding tables, the single asterik denotes this sample was diluted into the final molality of the immediately preceding sample.

Table 1. (Continued)

m_1	$n_2 \times 10^4$	$m_f^{\frac{1}{2}} \times 10^2$	$-q_{dil.}$ cal.	$\bar{P}_i$	$\emptyset_L(m_1)$ cal./mole
1.702	15.854	4.196	4.923		3369
	16.744*	6.014	5.038	5340	3370
	15.762	4.190	4.898		3371
1.948	14.042	3.948	4.880		3725
	14.895*	5.666	5.031	5560	3721
	14.813	4.061	5.133		3721
	15.012*	5.760	5.061	5470	3720
2.257	14.283	3.982	5.622		4188
	15.037*	5.703	5.776	5500	4186
	14.858	4.067	5.832		4181
2.552	13.932	3.932	6.144		4659
	14.407*	5.607	6.232	5250	4666
	14.161	3.970	6.250		4664
	14.391*	5.636	6.235	5150	4674
	12.516	3.727	5.552		4673
	12.714*	5.290	5.529	5550	4672
2.897	12.852	3.777	6.491		5290
	13.880*	5.445	6.890	5360	5295
	12.595	3.744	6.362		5289
	13.628*	5.401	6.753	5670	5284
3.250	11.583	3585	6.647		5968
	12.086*	5.124	6.840	5380	5974
	11.821	3.628	6.795		5980
	11.834*	5.129	6.702	5620	5978
3.590	9.303	3.213	6.030		6689
	10.029*	4.630	6.435	5160	6704
	9.033	3.170	5.848		6678
	11.253*	4.750	7.203	5090	6696
	8.740	3.118	5.680		6700
	8.855*	4.423	5.686	5840	6698
3.939	9.843	3.304	7.151		7478
	11.388*	4.852	8.162	6030	7467
	9.845	3.309			
	10.550	4.762	7.567		7467

Table 2. Observed heats of dilution of aqueous samarium chloride
solutions at 25°C.

m_1	$n_2 \times 10^4$	$m_f^{\frac{1}{2}} \times 10^2$	$-q_{dil.}$ cal.	$\bar{P}_i$	$\emptyset_L(m_1)$ cal./mole
0.09711	24.518	5.222	2.103		1178
0.1596	29.444	5.715	3.000		1365
	26.295	5.316	2.728		1361
0.2687	40.454	6.700	4.868		1599
	41.371	6.785	4.972		1602
0.3604	46.518	7.195	6.227		1758
0.5158	29.991	5.791	4.935		1996
	32.657*	8.341	4.960	4880	1991
	29.476	5.747	4.861		1997
	29.846*	8.127	4.565	4925	1992
0.6702	34.101	6.172	6.250		2202
	35.273*	8.777	6.012	4800	2195
	35.847	6.338	6.541		2203
	36.750*	8.992	6.263	4580	2204
0.8527	27.776	5.563	5.853		2446
	27.807*	7.855	5.554	4850	2448
	28.245	5.619	5.961		2452
	30.228*	8.069	6.036	4740	2457
1.063	24.025	5.178	5.734		2705
	24.318*	7.335	5.537	5060	2703
	23.500	5.120	5.627		2709
	23.788*	7.254	5.435	5090	2707
1.137	23.088	5.068	5.753		2804
	23.741*	5.197	5.644	5200	2798
	22.959	5.054	5.723		2804
	23.476*	7.180	5.586	5190	2799
1.437	19.336	4.642	5.624		3197
	19.293	4.636			
	19.922*	6.605	5.586		3195

Table 2. (Continued)

m_1	$n_2 \times 10^4$	$m_f^{\frac{1}{2}} \times 10^2$	$-q_{dil.}$cal.	$\bar{P}_i$	$\phi_L(m_1)$ cal./mole
1.666	17.586	4.420	5.693		3514
	18.805*	6.354	5.878	5530	3505
	17.455	4.404	5.658		3517
	17.722*	6.248	5.561	5440	3512
1.945	14.810	4.061	5.448		3935
	15.413*	5.799	5.523	5460	3934
2.116	14.070	3.952			
	14.842*	5.663	5.720		4197
	14.011	3.949	5.536		4201
	14.328*	5.615	5.532	5440	4202
2.523	11.483	3.575	5.349		4886
	11.852*	5.095	5.428	5380	4893
2.865	10.059	3.341	5.346		5529
	10.564*	4.782	5.529	5660	5531
3.179	9.106	3.183	5.407		6143
	9.393	3.233	5.575		6144
	9.806*	4.621	5.738	5910	6139
3.507	8.568	3.083			
	9.037*	4.418	5.932		6840
	8.199	3.016	5.437		6827
	8.710	3.108			
	8.810*	4.408	5.783		6840
3.641	8.717	3.110	6.028		7117
	9.284*	4.468	6.349	5730	7118
	7.480	2.884			
	8.963*	4.276	6.139		7117

Table 3. Observed heats of dilution of aqueous europium chloride solutions at 25°C.

m_1	$n_2 \times 10^4$	$m_f^{\frac{1}{2}} \times 10^2$	$-q_{dil.}$cal.	$\bar{P}_i$	$\emptyset_L(m_1)$ cal./mole
0.02154	3.044	1.837	0.187		735
	3.487	1.969	0.210		733
0.09530	14.264	3.977	1.336		1189
	14.667	4.038	1.366		1188
0.1662	23.251	5.078	2.552		1413
	23.910	5.157	2.613		1413
0.2819	37.358	6.438	4.787		1669
	35.802	6.311	4.622		1672
0.3866	35.953	6.316	5.307		1857
	42.427	6.871	6.134		1855
0.5187	26.164	5.411	4.541		2069
	30.592*	7.943	4.925	5000	2071
0.6733	26.138	5.400	5.130		2296
	30.412*	7.924	5.578	5080	2294
	25.732	5.366	5.045		2292
	30.097*	7.884	5.525	5010	2294
0.8286	28.324	5.619	6.146		2514
	29.869*	8.038	6.126	4960	2417
	27.129	5.506	5.907		2516
	27.879*	7.826	5.741	5070	2515
1.042	23.006	7.267	5.736		2808
	24.448*	5.619	5.823	5120	2811
1.182	20.628	4.790	5.621		3024
	24.240*	7.057	6.279	5630	3009
1.526	17.341	4.387	5.591		3501
	17.438*	6.209	5.451	5420	3502
	17.712	4.441	5.693		3494
	17.786*	6.284	5.553	5210	3501

Table 3. (Continued)

m_1	$n_2 \times 10^4$	$m_f^{\frac{1}{2}} \times 10^2$	$-q_{dil.}$ cal.	$\overline{P}_i$	$\emptyset_L(m_1)$ cal./mole
1.694	15.784	4.187	5.512		3758
	16.045	4.330	5.596		3762
	16.714*	6.037	5.647	5890	3746
1.980	14.892	4.066	5.882		4208
	15.036*	5.762	5.655	5580	4207
	14.614	4.034	5.782		4213
	15.293*	5.768	5.760	5620	4211
2.147	12.020	3.653	5.114		4488
	12.578*	5.223	5.220	6160	4474
	12.071	3.665	5.129		4484
	13.038*	5.285	5.421	5640	4484
2.573	12.645	3.746	6.322		5239
	12.664*	5.298	6.220	5660	5239
2.889	11.096	3.514	6.225		5836
	10.406*	4.891	5.672	5600	5840
3.066	8.208	3.017	4.933		6206
	8.858*	4.350	5.264	5470	6217
	8.235	3.027	4.947		6204
3.587	9.253	3.204	6.547		7284
	9.461*	4.556	6.621	5790	7285
	9.854	3.311	6.974		7291
	10.143*	4.716	7.091	5650	7286

Table 4. Observed heats of dilution of aqueous gadolinium chloride solutions at 25°C.

m_1	$n_2 \times 10^4$	$m_f^{1/2} \times 10^2$	$-q_{dil.}$ cal.	$\bar{P}_i$	$\emptyset_L(m_1)$ cal./mole
0.09913	18.990	4.596	1.770		1220
0.15933	32.711	6.024	3.442		1410
	34.019	6.152	3.559		1410
0.24836	49.109	7.383	5.870		1630
	53.263	7.700	6.286		1630
0.3590	26.149	5.413	3.969		1851
	29.455*	7.857	4.099	5120	1849
0.4448	27.566	5.560	4.564		1.997
	29.249*	7.953	4.492	5020	1998
0.6390	30.414	5.827	5.942		2309
	30.459*	8.221	5.568	5100	2302
0.8087	25.990	5.388	5.791		2561
	26.122*	7.616	5.536	4990	2565
0.9756	22.010	4.956	5.513		2813
	22.193*	7.014	5.314	5300	2811
1.209	19.871	4.688	5.699		3162
	20.351*	6.680	5.614	5420	3158
1.438	18.366	4.524	5.888		3491
	18.376*	6.394	5.709	5340	3492
1.524	17.116	4.361	5.766		3644
	17.761*	6.221	5.760	6120	3619
	15.772	4.183	5.334		3647
1.858	14.222	3.979	5.588		4182
	14.493*	5.652	5.561	5520	4184

Table 4. (Continued)

m_1	$n_2 \times 10^4$	$m_f^{\frac{1}{2}} \times 10^2$	$-q_{dil.}$cal.	$\bar{P}_i$	$\emptyset_L(m_1)$ cal./mole
2.148	12.953	3.792	5.753		4684
	14.044*	5.472	6.095	5860	4676
2.551	11.272	3.542	5.855		5422
	12.662*	5.159	6.465	5580	5426
2.868	9.832	3.303	5.725		6036
	10.458*	4.744	6.013	5410	6047
3.201	7.615	2.910	4.982		6732
	8.049*	4.174	5.196	6440	6720
	8.933	3.153	5.820		6720
	9.097*	4.479	5.861	5680	6724
3.436	8.361	3.045	5.893		7245
	8.415*	4.313	5.863	6130	7239
3.590	9.629	3.273	7.078		7562
	9.818*	4.651	7.131	6060	7555

Table 5. Observed heats of dilution of aqueous dysprosium chloride solutions at 25°C.

m_1	$n_2 \times 10^4$	$m_f^{\frac{1}{2}} \times 10^2$	$-q_{dil.}$ cal.	$\bar{P}_i$	$\emptyset_L(m_1)$ cal./mole
0.04234	8.997	3.158	0.667		943
	10.131	3.352	0.733		937
	9.684	3.281	0.714		947
0.09126	19.192	4.614	1.751		1197
	17.265	4.382	1.602		1200
0.1668	28.466	5.620	3.153		1446
	31.978	5.965	3.494		1448
0.2369	35.274	6.256	4.395		1616
	38.092	6.511	4.707		1618
0.3649	12.708	3.762	2.066		1863
	12.091*	5.246	1.879	5160	1873
0.5647	16.606	4.298	3.240		2219
	16.729*	6.079	3.102	5340	2215
0.9741	19.046	4.605	4.911		2863
	18.629	6.470	4.620	5240	2861
1.163	16.708	4.312	4.829		3159
	16.862*	6.107	4.702	5450	3151
1.443	12.838	3.776	4.328		3610
	13.069*	5.361	4.297	5340	3613
1.669	18.523	4.540			
	19.459*	6.497	7.019		3988
	12.364	3.705	4.653		3998
	12.811*	5.285	4.693	5920	3983
	10.770	3.460	4.069		3999
	11.051*	4.923	4.077	5840	3991

Table 5. (Continued)

m_1	$n_2 \times 10^4$	$m_f^{\frac{1}{2}} \times 10^2$	$-q_{dil.}$ cal.	$\bar{P}_i$	$\emptyset_L(m_1)$ cal./mole
1.910	14.946	4.076			
	14.854*	5.754	6.040		4411
	9.732	3.286	4.104		4428
	9.753*	4.648	4.034	5810	4423
	9.001	3.160	3.794		4418
	9.159*	4.487	3.799	5400	4425
2.172	9.642	3.273	4.526		4904
	9.806*	4.647	4.529	5570	4906
	8.235	3.021	3.883		4909
2.494	9.569	3.259	5.081		5518
	10.104*	4.614	5.289	5600	5520
2.783	10.107	3.349	5.975		6126
	6.155	2.613	3.663		6122
	7.831*	3.937	4.606	5480	6130
3.098	7.677	2.919	5.079		6804
	8.873*	4.284	5.782	6550	6784
3.631	7.576	2.899	5.875		7943
	8.419*	4.211	6.472	5560	7949
	6.851	2.759	5.329		7957
	7.094*	3.935	5.471	5750	7959

Table 6. Observed heats of dilution of aqueous erbium chloride solutions at 25°C.

m_1	$n_2 \times 10^4$	$m_f^{1/2} \times 10^2$	$-q_{dil.}$ cal.	$\bar{P}_i$	$\emptyset_L(m_1)$ cal./mole
0.04584	9.414	3.231	0.708		962
	8.545	3.082	0.645		956
0.08689	14.685	4.035	1.340		1170
	17.095	4.361	1.523		1167
0.1674	26.238	5.393	2.899		1439
	24.983	5.268	2.776		1438
0.2666	58.731	8.075	7.047		1670
	58.733	8.087	7.049		1671
0.3874	25.926	5.389	4.065		1902
	26.876*	7.662	3.906	5100	1904
	26.957	5.499	4.210		1902
	29.332*	7.912	4.224	5080	1903
0.4764	31.153	5.907	5.281		2057
	35.719*	8.618	5.579	4930	2058
	33.910	6.167	5.698		2056
	34.876*	8.748	5.423	4880	2057
0.6311	32.822	6.056	6.352		2305
	34.251*	8.631	6.184	4990	2302
	30.659*	5.859	5.959		2303
	31.195	8.299	5.685	4990	2304
0.8723	16.985	4.346	4.073		2673
	17.271*	6.165	3.973	5430	2676
	16.892	4.340	4.048		2671
	17.383*	6.175	4.003	5290	2678
1.030	19.669	4.669	5.153		2914
	20.139*	6.647	5.062	5390	2914
	19.895	4.710	5.203		2911
	20.136*	6.675	5.059	5310	2914
1.218	14.031	3.948	4.137		3201
	14.084*	5.585	4.024	5610	3201
	13.866	3.930	4.087		3199
	14.293*	5.597	4.087	5450	3205

Table 6. (Continued)

m_1	$n_2 \times 10^4$	$m_f^{\frac{1}{2}} \times 10^2$	$-q_{dil.}$ cal.	$\overline{P}_i$	$\emptyset_L(m_1)$ cal./mole
1.453	13.403	3.858	4.456		3572
	13.978*	5.511	4.517	5640	3572
	13.784	3.918	4.576		3570
	14.208*	5.580	4.590	5510	3575
1.805	11.678	3.601	4.581		4155
	11.972*	5.122	4.602	5460	4163
	11.131	3.520	4.377		4160
	11.532*	5.021	4.447	5430	4170
2.067	11.709	3.605	5.131		4614
	11.904*	5.118	5.106	5930	4608
	11.483	3.575	5.023		4605
	11.795*	5.088	5.062	5600	4609
2.343	9.859	3.307	4.835		5118
	10.915	3.485	5.339		5117
	11.167*	4.956	5.367	5810	5116
2.695	9.814	3.300	5.487		5805
	11.121*	4.819	6.131	5470	5815
2.904	10.509	3.415	6.298		6214
	10.829*	4.865	6.322	5460	6224
	10.264	3.379	6.166		6226
	10.627*	4.820	6.303	5560	6233
3.222	، 8.054	2.989	5.399		6898
	8.694*	4.310	5.769	5510	6909
	7.942	2.972	5.331		6905
	8.081*	4.221	5.368	5730	6911
3.535	7.637	2.911	5.638		7573
	7.644*	4.117	5.606	5010	7596
	،6.738	2.738	4.982		7572
	7.227*	3.941	5.308	5000	7596
3.782	9.999	3.331			
	10.287*	4.743	8.034		8107
	10.235	3.375	8.096		8129
	10.483*	4.800	8.214	5510	8137

Table 7. Observed heats of dilution of aqueous thulium chloride
solutions at 25°C.

m_1	$n_2 \times 10^4$	$m_f^{\frac{1}{2}} \times 10^2$	$-q_{dil.}$ cal.	$\bar{P}_i$	$\emptyset_L(m_1)$ cal./mole
0.03809	6.692	2.724	0.477		890
	7.093	2.803	0.502		890
0.08727	14.521	4.013	1.318		1160
	18.160	4.494	1.603		1162
0.1638	28.268	5.600	3.042		1413
	24.384	5.208	2.670		1412
0.2801	9.369	3.228	1.376		1675
	9.895*	4.620	1.385	5280	1686
	8.652	3.109	1.283		1683
	9.348*	4.476	1.313	5680	1683
0.3700	14.374	4.001	2.295		1848
	14.619*	5.671	2.205	5310	1850
	12.908	3.799			
	14.696*	5.542	2.228		1852
0.5156	19.293	4.636	3.483		2092
	20.721	4.815	3.724		2094
	20.716*	6.793	3.520	5010	2095
0.6405	18.911	4.588	3.796		2291
	19.932*	6.564	3.785	5320	2285
	19.149	4.625	3.844		2293
	19.563*	6.565	3.714	5380	2284
0.8232	17.378	4.396	3.962		2553
	17.897*	6.255	3.912	5170	2556
	17.724	4.448	4.051		2562
	18.041*	6.311	3.936	5400	2555
1.037	17.543	4.416	4.577		2883
	18.098*	6.288	4.533	5400	2876
	17.906	4.437	4.661		2878
	18.479*	6.366	4.634	5150	2883
1.458	16.306	4.256	5.309		3521
	16.844*	6.064	5.333	5120	3527
	16.622	4.305	5.418		3528
	17.080*	6.126	5.399	5340	3525
1.712	15.767	4.184	5.816		3950
	16.940*	6.023	6.071	5530	3942
	16.210	4.246			
	16.616*	6.039	5.946		3938

Table 7. (Continued)

m_1	$n_2 \times 10^4$	$m_f^{\frac{1}{2}} \times 10^2$	$-q_{dil.}$ cal.	$\overline{P}_i$	$\emptyset_L(m_1)$ cal./mole
1.953	14.060	3.950	5.754		4341
	15.056*	5.682	6.027	5280	4345
	14.660	4.035	6.006		4350
	15.304*	5.766	6.122	5500	4346
2.225	12.656	3.747	5.796		4816
	12.294	3.697			
	12.921*	5.292	5.811		4819
2.599	9.510	3.248	5.048		5516
	9.558*	4.598	5.011	5260	5527
	8.747	3.117	5.649		5515
	9.895*	4.550	5.179	5710	5515
2.916	8.910	3.144			
	8.740*	4.424	5.142		6158
	8.973	3.157	5.339		6153
	9.266*	4.501	5.444	5660	6155
3.328	6.612	2.708	4.519		7010
	6.814*	3.858	4.611	5930	7010
	7.474	2.881	5.097		7006
	8.041*	4.151	5.421	6030	7001
3.620	6.132	2.608	4.566		7617
	6.527*	3.746	4.812	6670	7608
	6.921	2.773	5.141		7608
	7.072*	3.942	5.214	5260	7621
3.700	7.972	2.974	6.112		7858
	8.033*	4.213	6.083	6670	7836
	7.442	2.877	5.702		7847
	7.950*	4.137	6.037	5600	7852
3.881	7.649	2.913	6.150		8229
	7.491	2.885	6.018		8220
	8.698*	4.240	6.926	5530	8228

Table 8. Observed heats of dilution of aqueous lutetium chloride solutions at 25°C.

m_1	$n_2 \times 10^4$	$m_f^{\frac{1}{2}} \times 10^2$	$-q_{dil.}$ cal.	$\overline{P}_i$	$\emptyset_L(m_1)$ cal./mole
0.01119	1.714	1.378	0.0855		591
	1.943	1.470	0.0902		563
0.04102	5.167	2.393	0.385		902
	6.534	2.695	0.471		897
0.09044	13.078	3.808	1.204		1163
	11.564	3.586	1.086		1168
0.1625	27.823	5.555	2.959		1403
	24.798	5.253	2.678		1403
	30.201	5.788	3.152		1395
	22.149	4.964	2.410		1395
	16.221	4.242	1.843		1403
	16.409	4.271	1.871		1409
0.2519	11.806	4.918	1.554		1621
	25.283	5.295	3.263		1616
	30.020	5.780	3.811		1620
0.4324	27.844*	5.583	4.472		1947
	30.594	8.056	5.536	4980	1944
	25.309	5.333			
	27.416*	7.670	4.111		1944
0.5036	17.879	4.465	3.201		2070
	20.624*	6.537	3.463	5350	2068
	16.030	4.231	2.875		2060
	17.047*	6.066	2.888	5410	2060
0.6487	21.343	4.876	4.236		2287
	22.483*	6.974	4.215	5220	2286
	20.392	4.783	4.047		2282
	23.577*	7.008	4.411	5160	2283
0.7963	20.206	4.742	4.467		2506
	22.163*	6.856	4.641	5390	2499
	21.212	4.868	4.652		2495
	19.249	4.624	4.274		2509
	23.578*	6.894	4.954	5260	2508
	19.835	4.706			
	22.257*	6.845	4.683		2509
1.002	28.073	5.593	6.923		2807
	32.740*	8.217	7.652	4910	2806
	33.822	6.151	8.247		2808
	19.429	4.648	4.893		2808

Table 8. (Continued)

m_1	$n_2 \times 10^4$	$m_f^{\frac{1}{2}} \times 10^2$	$-q_{dil.}$ cal.	$\overline{P}_i$	$\emptyset_L(m_1)$ cal./mole
1.002 (Continued)					
	19.583*	6.579	4.732	5290	2808
	19.480	4.662	4.906		2808
	19.990*	6.632	4.833	5190	2812
1.215	17.680	4.432	5.030		3123
	17.709*	6.266	4.870	5290	3125
	17.350	4.398	4.935		3120
	18.202	6.291	4.997	5290	3122
1.478	21.103	4.843	6.787		3517
	21.767*	6.897	6.772	5150	3518
	21.232	4.866	6.826		3517
	22.083*	6.946	6.866	5140	3519
1.719	20.876	4.816	7.504		3894
	22.089*	6.905	7.711	5090	3896
	19.779	4.695	7.127		3896
	20.137*	6.666	7.044	5310	3895
1.999	11.380	3.554	4.706		4363
	13.516	3.880			
	14.032*	5.537	5.643		4359
2.249	10.155	3.357	4.639		4784
	10.290	3.384	4.689		4774
	10.816*	4.846	4.844	5530	4779
2.569	8.407	3.072	4.340		5362
	10.252*	4.549	5.182	6640	5339
	9.853	3.311	5.074		5363
2.917	7.239	2.834	4.223		6018
	7.539*	4.048	4.341	6090	6014
	8.063	2.995	4.689		6009
	8.606*	4.306	4.945	5560	6017
3.086	7.948	2.969	4.893		6343
	8.318*	4.247	5.059	5850	6349
	8.461	3.068	5.221		6370
	9.508*	4.470	5.791	5800	6370
3.307	9.049	3.169	5.987		6820
	10.604*	4.669	6.927	5660	6824
	8.648	3.102	5.720		6815
	8.905*	4.418	5.830	5480	6824

Table 8. (Continued)

m_1	$n_2 \times 10^4$	$m_f^{\frac{1}{2}} \times 10^2$	$-q_{dil.}$ cal.	$\bar{P}_i$	$\emptyset_L(m_1)$ cal./mole
3.913	6.677	2.721	5.288		8097
	6.526	2.694	5.183		8118
4.128	6.806	2.748			
	7.116*	3.929	5.899		8539
	6.265	2.640	5.234		8527

Table 9. Parameters for the empirical expressions of $\bar{P}_i$ and $\emptyset_L$ below 0.007 molal corresponding to equations 7.6 and 7.7

	A	B
NdCl$_3$	6925	-15330
SmCl$_3$	6925	-15150
EuCl$_3$	6925	-14070
GdCl$_3$	6925	-13990
DyCl$_3$	6925	-14560
ErCl$_3$	6925	-13580
TmCl$_3$	6925	-16060
LuCl$_3$	6925	-14810

Table 10. Parameters for the empirical expressions of $\emptyset_L$ below 0.25 molal corresponding to equation 7.9

	b	c	d	e
NdCl$_3$	7007.0	-18844.0	33186.9	-22740.0
SmCl$_3$	6915.7	-16603.5	25786.5	-15437.8
EuCl$_3$	7015.5	-17566.1	29615.3	-19318.3
GdCl$_3$	6945.3	-15856.5	23471.1	-12939.0
DyCl$_3$	6927.1	-15864.4	24874.3	-15283.3
ErCl$_3$	7050.0	-17413.7	29170.4	-18882.7
TmCl$_3$	6851.2	-16191.8	26079.7	-16255.1
LuCl$_3$	7029.4	-18450.1	33269.8	-23136.6

Table 11. Parameters for the empirical expressions of $\emptyset_L$ above 0.25 molal corresponding to equation 7.10

	a'	b'	c'	d'	e'
NdCl$_3$	588.70	2101.60	-596.02	141.34	256.28
SmCl$_3$	182.07	3788.14	-2815.90	1508.91	-39.06
EuCl$_3$	125.82	4180.22	-3484.37	2146.88	-223.66
GdCl$_3$	283.66	3538.88	-2440.69	1557.25	-97.08
DyCl$_3$	262.01	3768.19	-2965.70	2066.18	-228.32
ErCl$_3$	215.97	3844.14	-2959.29	1957.54	-193.32
TmCl$_3$	398.20	3101.74	-2002.86	1414.68	-88.49
LuCl$_3$	410.82	3021.44	-1879.21	1333.97	-84.84

Table 12. Relative partial molal heat contents and relative partial molal excess entropies of aqueous neodymium chloride solutions at 25°C.

Molality	$-\bar{L}_1$ cal./mole	$\bar{L}_2$ cal./mole	$-T(\bar{S}_1-\bar{S}_1{}^o)$ cal./mole	$T(\bar{S}_2-\bar{S}_2{}^o)$ cal./mole
0.1	0.618	1496	1.56	4176
0.2	1.53	1847	2.93	4821
0.5	5.84	2539	6.00	5606
1.0	21.2	3671	12.9	6114
1.5	52.3	5040	19.6	6480
2.0	106	6738	32.4	6960
2.5	190	8794	62.1	7758
3.0	311	11228	119	8981
3.5	466	14046	212	10646
3.929	659	16775	330	12443

Table 13. Relative partial molal heat contents and relative partial molal excess entropies of aqueous samarium chloride solutions at 25°C.

Molality	$-\bar{L}_1$ cal./mole	$\bar{L}_2$ cal./mole	$-T(\bar{S}_1-\bar{S}_1{}^0)$ cal./mole	$T(\bar{S}_2-\bar{S}_2{}^0)$ cal./mole
0.1	0.626	1535	1.55	4191
0.2	1.59	1902	2.96	4844
0.5	5.94	2635	6.08	5649
1.0	20.1	3738	11.2	6099
1.5	48.7	5084	15.0	6421
2.0	97.7	6731	22.1	6819
2.5	172	8673	41.9	7488
3.0	276	10896	82.3	8494
3.5	414	13384	148	9819
3.641	460	14133	183	10260

Table 14. Relative partial molal heat contents and relative partial molal excess entropies of aqueous europium chloride solutions at 25°C.

Molality	$-\bar{L}_1$ cal./mole	$\bar{L}_2$ cal./mole	$-T(\bar{S}_1-\bar{S}_1{}^o)$ cal./mole	$T(\bar{S}_2-\bar{S}_2{}^o)$ cal./mole
0.1	0.669	1576	1.56	4209
0.2	1.71	1975	3.03	4874
0.5	6.87	2805	7.00	5788
1.0	24.8	4124	15.4	6422
1.5	60.6	5703	25.6	6945
2.0	119	7543	37.0	7051
2.5	204	9640	70.3	8300
3.0	317	11930	119	9348
3.5	462	14390	190	10623
3.587	611	14832	205	10870

Table 15. Relative partial molal heat contents and relative partial molal excess entropies of aqueous gadolinium chloride solutions at 25°C.

Molality	$-\bar{L}_1$ cal./mole	$\bar{L}_2$ cal./mole	$-T(\bar{S}_1-\bar{S}_1^{\,o})$ cal./mole	$T(\bar{S}_2-\bar{S}_2^{\,o})$ cal./mole
0.1	0.661	1591	1.57	4225
0.2	1.75	2001	3.08	4912
0.5	7.29	2901	7.41	5853
1.0	26.5	4315	16.6	6550
1.5	63.9	5965	27.6	7112
2.0	125	7885	44.5	7720
2.5	213	10058	76.0	8564
3.0	333	12464	129	9702
3.5	486	15085	208	11116
3.590	518	15577	226	11402

Table 16. Relative partial molal heat contents and relative partial molal excess entropies of aqueous dysprosium chloride solutions at 25°C.

Molality	$-\bar{L}_1$ cal./mole	$\bar{L}_2$ cal./mole	$-T(\bar{S}_1-\bar{S}_1{}^\circ)$ cal./mole	$T(\bar{S}_2-\bar{S}_2{}^\circ)$ cal./mole
0.1	0.690	1621	1.59	4313
0.2	1.73	2019	3.06	4992
0.5	7.40	2948	7.50	5932
1.0	28.1	4463	17.5	6697
1.5	68.3	6236	30.1	7328
2.0	132	8263	47.9	7969
2.5	223	10508	76.3	8815
3.0	344	12933	130	9903
3.5	495	15509	202	11205
3.631	539	16204	226	11592

Table 17. Relative partial molal heat contents and relative partial molal excess entropies of aqueous erbium chloride solutions at 25°C.

Molality	$-\bar{L}_1$ cal./mole	$\bar{L}_2$ cal./mole	$-T(\bar{S}_1-\bar{S}_1{}^o)$ cal./mole	$T(\bar{S}_2-\bar{S}_2{}^o)$ cal./mole
0.1	0.683	1601	1.60	4257
0.2	1.75	2010	3.04	4926
0.5	7.39	2919	7.49	5842
1.0	27.2	4377	16.4	6537
1.5	65.9	6086	26.8	7072
2.0	128	8056	42.3	7641
2.5	218	10257	69.5	8381
3.0	337	12657	115	9361
3.5	487	15229	181	10564
3.782	587	16746	231	11354

Table 18. Relative partial molal heat contents and relative partial molal excess entropies of aqueous thulium chloride solutions at 25°C.

Molality	$-\bar{L}_1$ cal./mole	$\bar{L}_2$ cal./mole	$-T(\bar{S}_1-\bar{S}_1{}^o)$ cal./mole	$T(\bar{S}_2-\bar{S}_2{}^o)$ cal./mole
0.1	0.675	1586	1.55	4160
0.2	1.79	1990	3.08	4842
0.5	7.18	2869	7.29	5733
1.0	27.8	4316	16.8	6405
1.5	66.2	5988	26.9	6904
2.0	126	7908	39.6	7398
2.5	213	10061	63.6	8078
3.0	330	12427	106	9010
3.5	480	14988	170	10166
3.881	620	17062	238	11211

Table 19. Relative partial molal heat contents and relative partial molal excess entropies of aqueous lutetium chloride solutions at 25°C.

Molality	$-\bar{L}_1$ cal./mole	$\bar{L}_2$ cal./mole	$-T(\bar{S}_1-\bar{S}_1{}^0)$ cal./mole	$T(\bar{S}_2-\bar{S}_2{}^0)$ cal./mole
0.1	0.688	1580	1.54	4044
0.2	1.75	1990	3.10	4744
0.5	7.16	2852	7.25	5611
1.0	26.3	4265	15.5	6259
1.5	62.8	5878	23.6	6694
2.0	121	7718	33.7	7090
2.5	205	9772	54.2	7661
3.0	316	12023	90.1	8452
3.5	459	14454	144	9440
4.0	634	17048	221	10623
4.128	684	17736	241	10944

Table 20. Parameters for the empirical expressions of $\bar{L}_1$ below 0.25 molal corresponding to equation 7.11

	D	E	F	G
NdCl$_3$	63.142	-339.74	897.57	-820.05
SmCl$_3$	62.334	-299.41	697.51	-556.75
EuCl$_3$	63.223	-316.67	800.85	-696.40
GdCl$_3$	62.619	-286.12	635.48	-467.25
DyCl$_3$	62.452	-286.23	673.30	-551.63
ErCl$_3$	63.501	-313.70	788.26	-680.38
TmCl$_3$	54.646	-211.88	420.20	-262.69
LuCl$_3$	63.301	-332.21	898.56	-833.20

Table 21. Parameters for the empirical expressions of $\bar{L}_2$ below 0.25 molal corresponding to equation 7.12

	A'	B'	C'	D'	E'
NdCl$_3$	0	10510.0	-37688.0	82964.0	-68217.0
SmCl$_3$	0	10374.0	-33207.0	64468.0	-46314.0
EuCl$_3$	0	10523.0	-35132.0	74042.0	-57954.0
GdCl$_3$	0	10418.0	-31713.0	58677.0	-38817.0
DyCl$_3$	0	10391.0	-31729.0	62186.0	-45850.0
ErCl$_3$	0	10534.0	-34459.0	71881.0	-55704.0
TmCl$_3$	0	10277.0	-32383.0	65200.0	-48767.0
LuCl$_3$	0	10544.0	-36903.0	83183.0	-69419.0

Table 22. Parameters for the empirical expressions of $\bar{L}_1$ above 0.25 molal corresponding to equation 7.11

	D	E	F	G
NdCl$_3$	18.882	-10.631	3.746	9.2502
SmCl$_3$	34.181	-50.875	38.188	-1.4366
EuCl$_3$	37.671	-62.812	58.045	-8.0657
GdCl$_3$	31.898	-44.020	42.120	-3.4620
DyCl$_3$	32.132	-49.727	53.370	-7.6903
ErCl$_3$	34.636	-53.339	52.923	-6.9719
TmCl$_3$	14.453	-1.8518	12.218	2.9937
LuCl$_3$	28.135	-36.228	37.946	-3.5288

Table 23. Parameters for the empirical expressions of $\bar{L}_2$ above 0.25 molal corresponding to equation 7.12

	A'	B'	C'	D'	E'
NdCl$_3$	588.58	3152.9	-1192.7	353.7	768.77
SmCl$_3$	182.22	5681.6	-5631.0	3621.8	-117.09
EuCl$_3$	126.17	6268.9	-6966.6	5365.9	-670.68
GdCl$_3$	283.61	5308.4	-4881.4	3893.1	-288.70
DyCl$_3$	291.05	5550.9	-5805.1	5098.5	-672.14
ErCl$_3$	215.63	5767.6	-5920.6	4895.0	-580.20
TmCl$_3$	418.37	4582.4	-3918.5	3490.6	-256.67
LuCl$_3$	410.69	4532.7	-3759.2	3335.4	-254.62

Table 24. Observed heats of solution of rare-earth chloride hydrates in water at 25°C.

	$n_2 \times 10^4$	$m_f^{\frac{1}{2}} \times 10^2$	$-q_{sol}$.cal.	$\bar{L}^{\cdot}$ cal./mole
$LaCl_3 \cdot 7H_2O$	10.451	3.403	6.762	6688
	14.690*	5.278	9.329	6673
	12.503	3.728	8.071	6692
	12.662*	5.288	8.054	6684
$PrCl_3 \cdot 7H_2O$	14.416	3.998	9.737	7006
	16.546*	5.859	10.984	6989
	15.059	4.092	10.160	7003
	15.943*	5.871	10.601	7000
$NdCl_3 \cdot 6H_2O$	8.389	3.049	7.513	9154
	11.250	3.536	10.003	9119
	14.005*	5.297	12.328	9129
$SmCl_3 \cdot 6H_2O$	6.529	2.690	5.499	8597
	7.818*	3.987	6.544	8622
	6.617	2.712	5.580	8610
	8.325*	4.075	6.962	8619
$EuCl_3 \cdot 6H_2O$	12.202	3.682	10.348	8716
	13.166*	5.308	11.021	8699
$GdCl_3 \cdot 6H_2O$	7.035	2.792	6.290	9124
	10.237*	4.375	9.035	9102
	8.698	3.109	7.752	9114
	9.209*	4.461	8.120	9109
$DyCl_3 \cdot 6H_2O$	8.518	3.073	8.330	9978
	9.166*	4.427	8.860	9944
	8.152	3.010	7.959	9958
	9.254*	4.398	8.957	9956
$ErCl_3 \cdot 6H_2O$	5.807	2.537	6.137	10735
$TmCl_3 \cdot 6H_2O$	8.827	3.128	9.631	11112
$YbCl_3 \cdot 6H_2O$	5.950	2.568	6.756	11523
	6.867*	3.769	7.711	11469
	6.263	2.638		
	6.619*	3.784	7.456	11504
$LuCl_3 \cdot 6H_2O$	6.972	2.780	8.132	11845
	9.997	4.336	11.592	11868
	4.994	2.356	5.835	11839
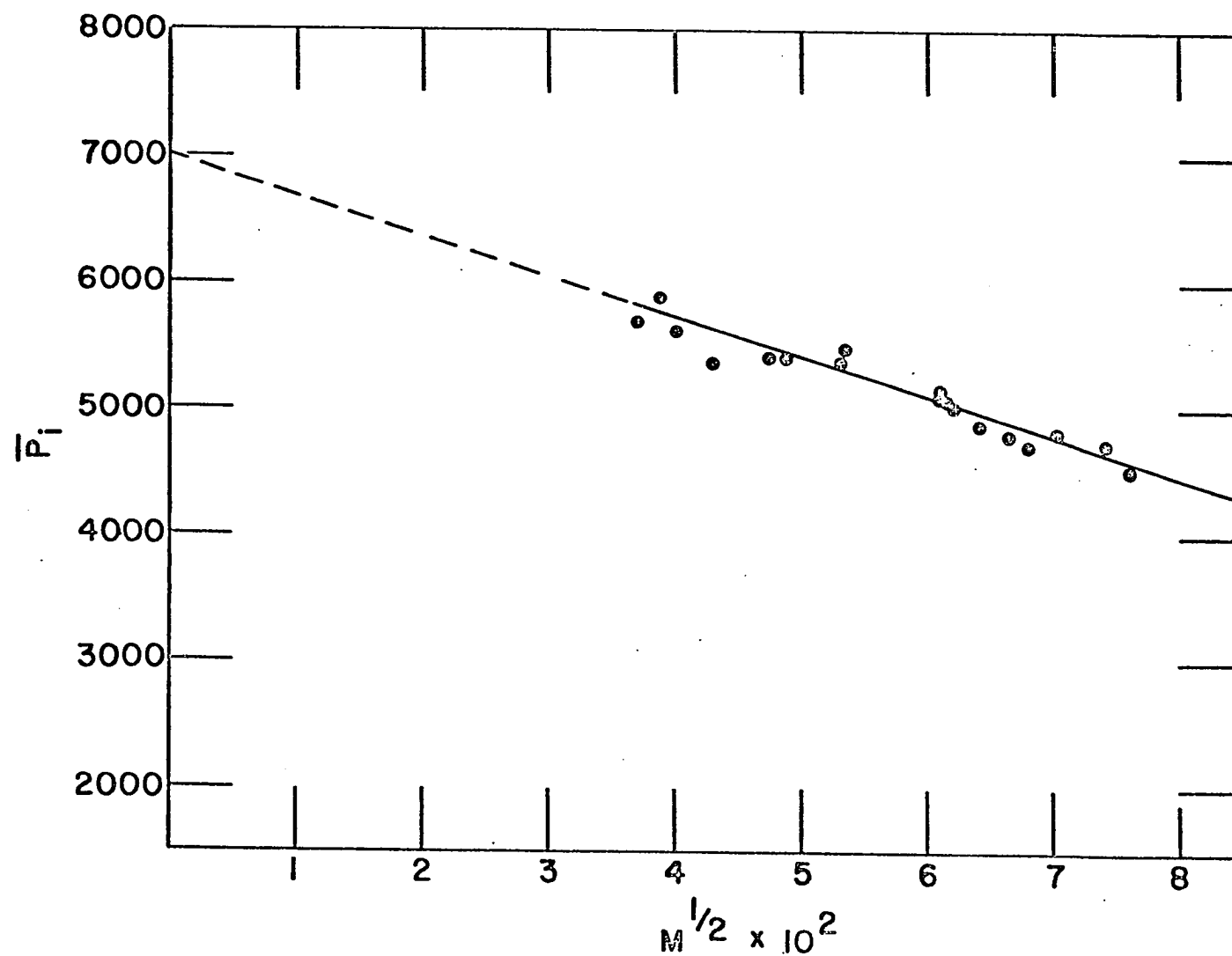
Figure 4. $\bar{P}_i$ versus $m^{1/2}$ for samarium chloride solutions at 25°C.

88
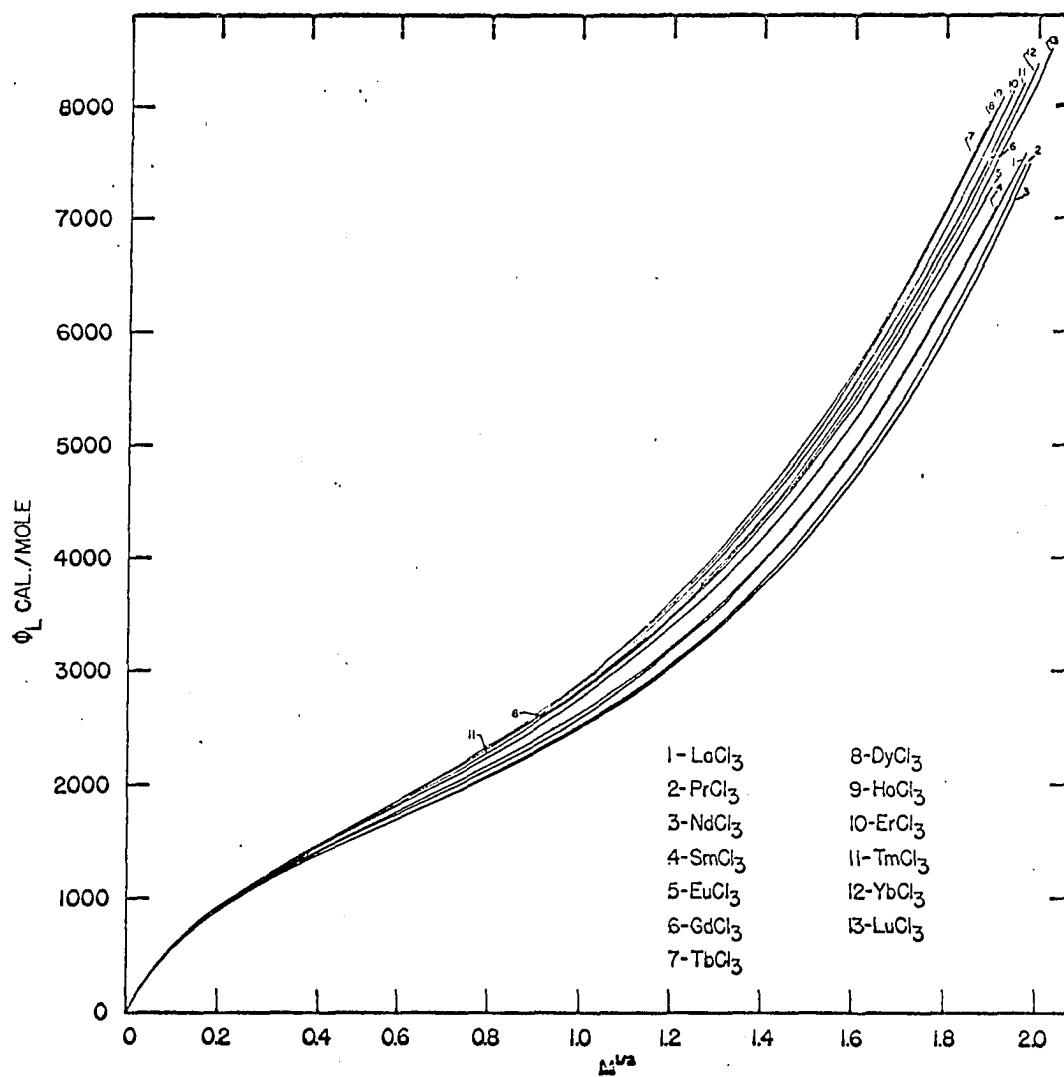
Figure 5. Relative apparent molal heat contents of thirteen aqueous rare-earth chloride solutions versus $m^{1/2}$ at 25°C.
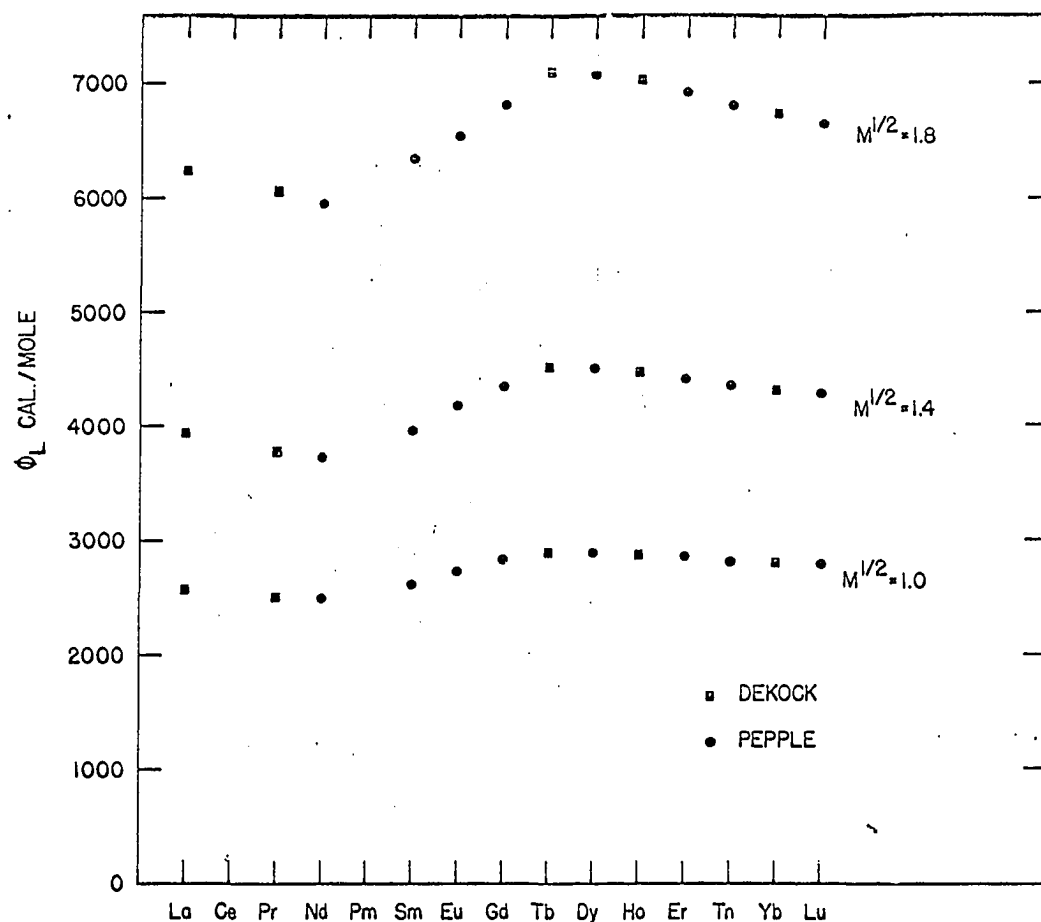
Figure 6. Relative apparent molal heat contents of thirteen rare-earth chloride solutions at three values of $m^{1/2}$ at 25°C.
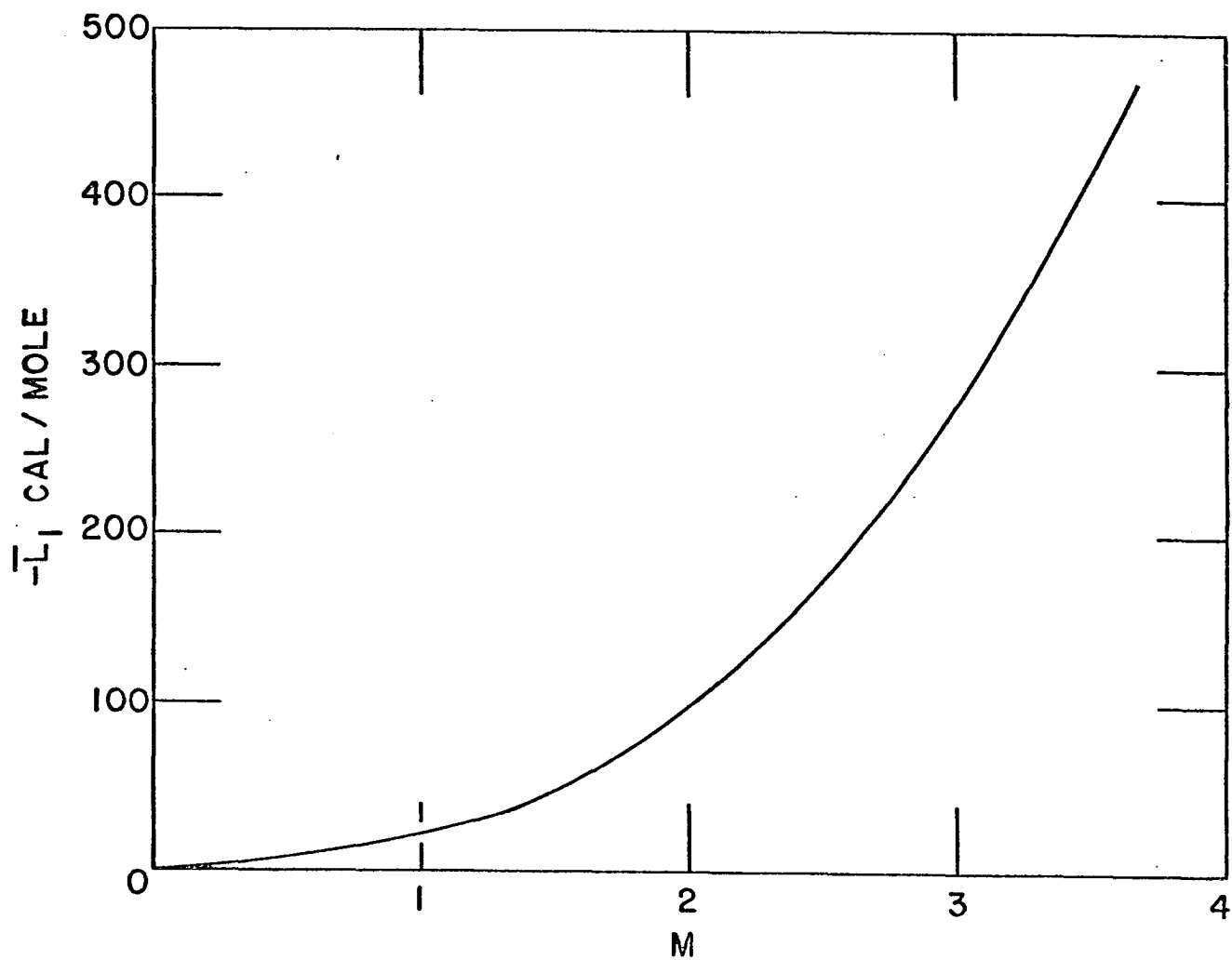
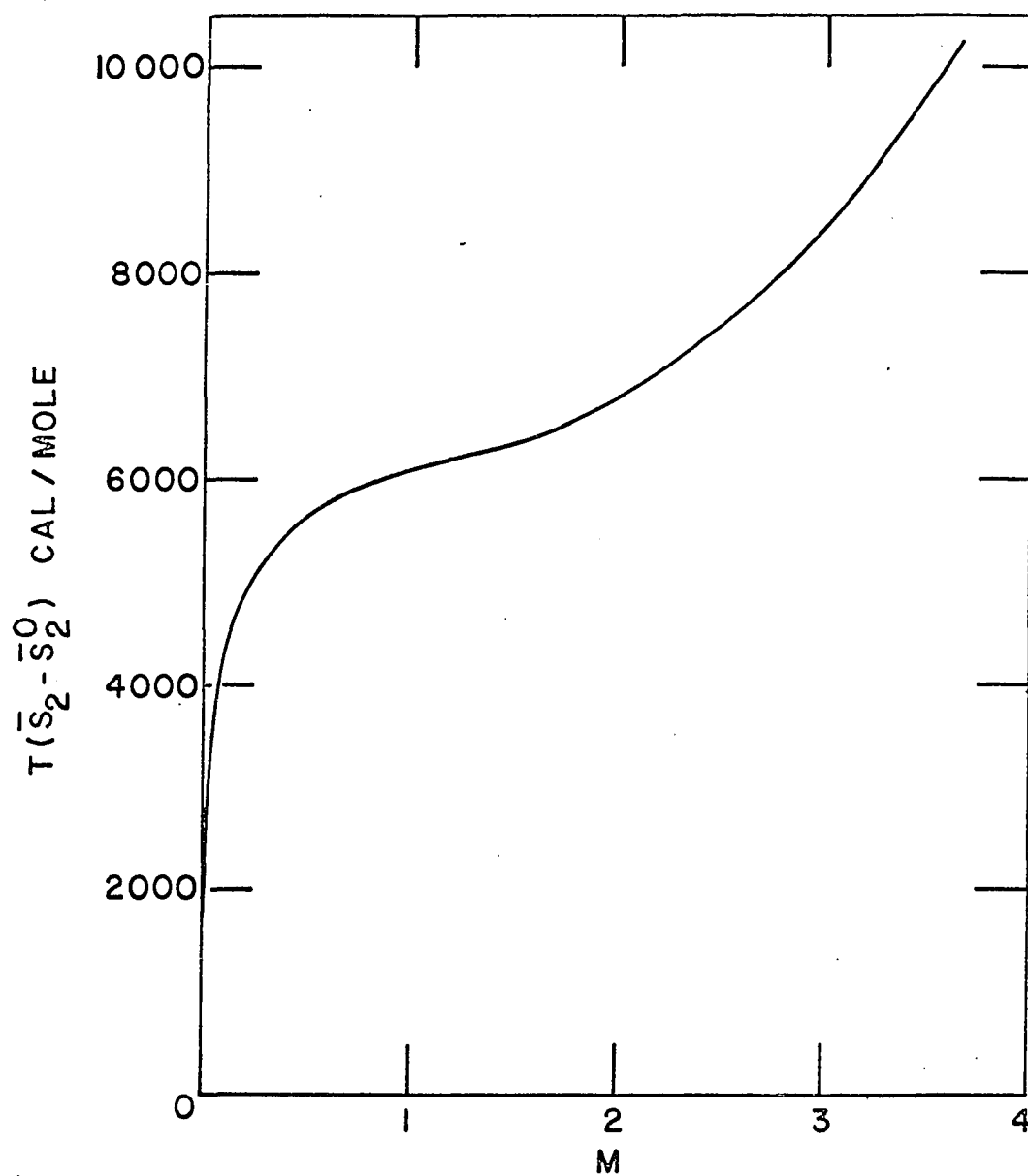Figure 7. Relative partial molal heat contents of water in aqueous samarium chloride solutions versus molality at 25°C.
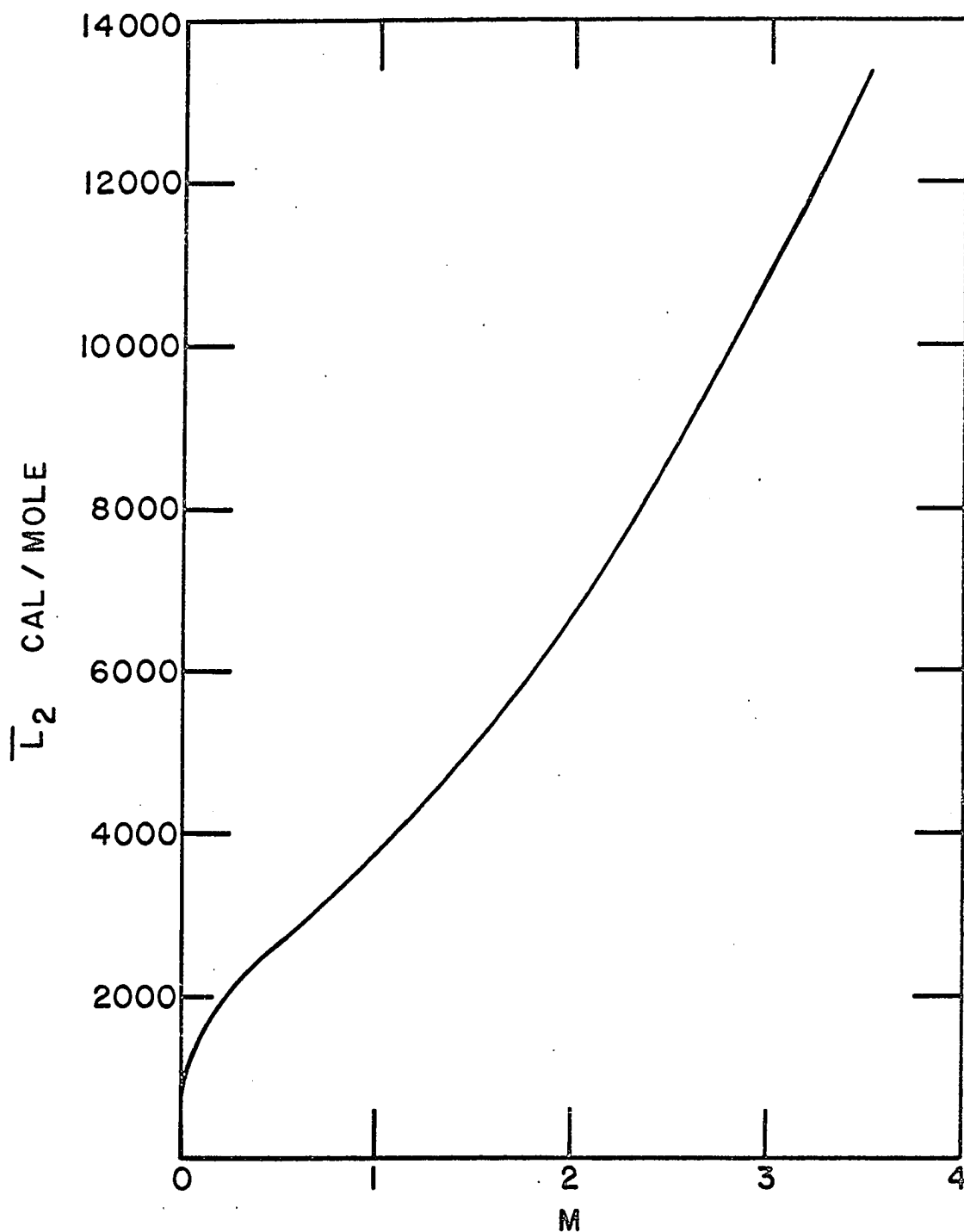
Figure 8. Relative partial molal heat contents of the solute in aqueous samarium chloride solutions versus molality at 25°C.
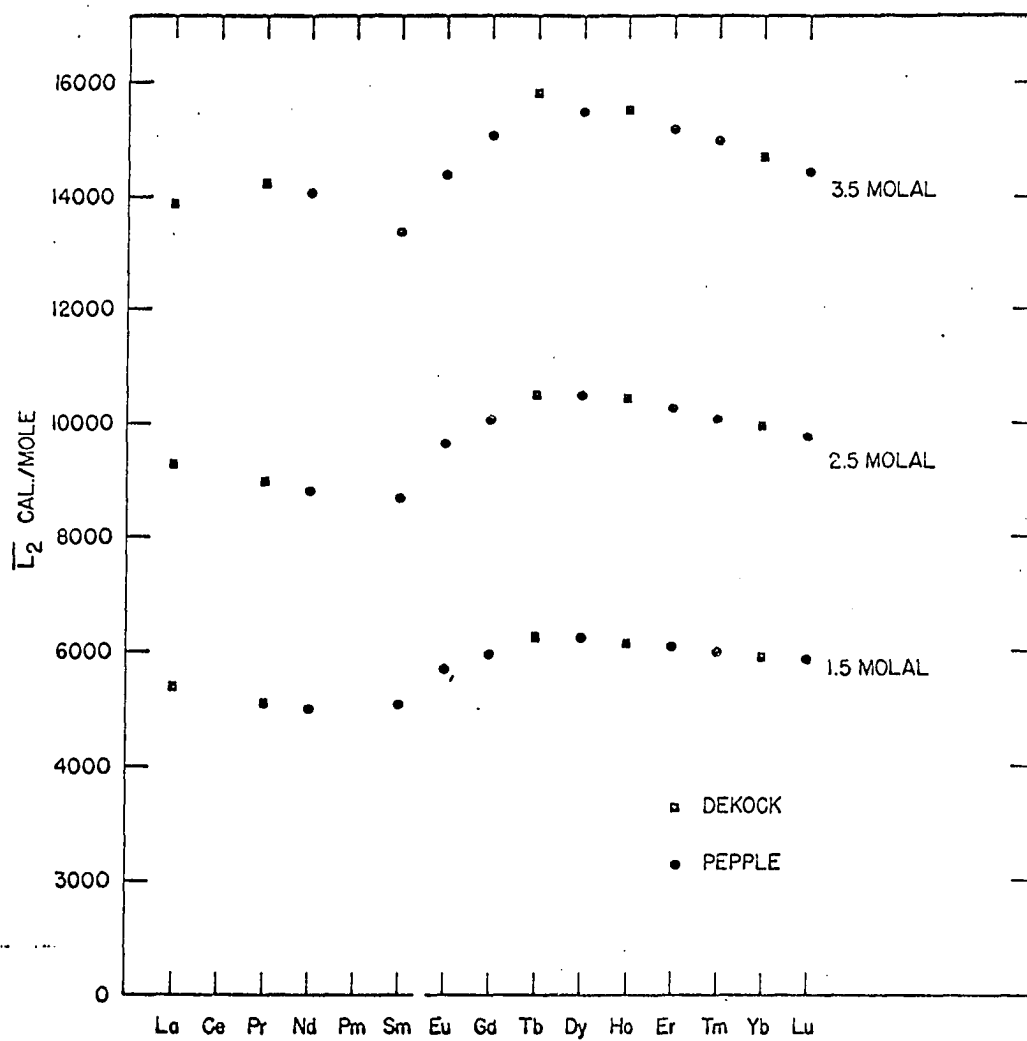
Figure 9. Relative partial molal heat contents of the solute
in thirteen aqueous rare-earth chloride solutions
at three values of m at 25°C.
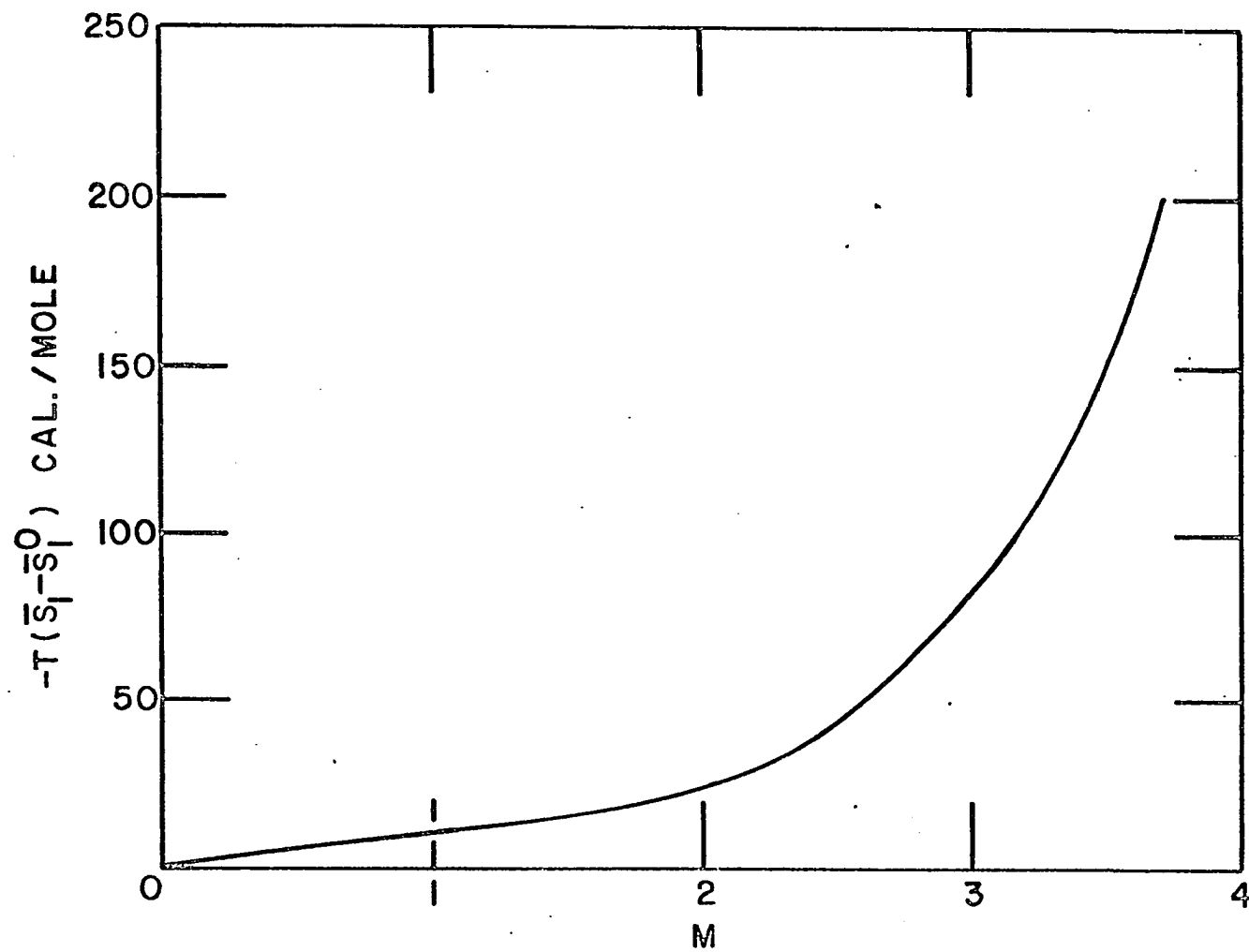
Figure 10. Relative partial molal excess entropies of water in aqueous samarium chloride solutions at 25°C.

Figure 11. Relative partial molal excess entropies of the
solute in aqueous samarium chloride solutions
at 25°C.
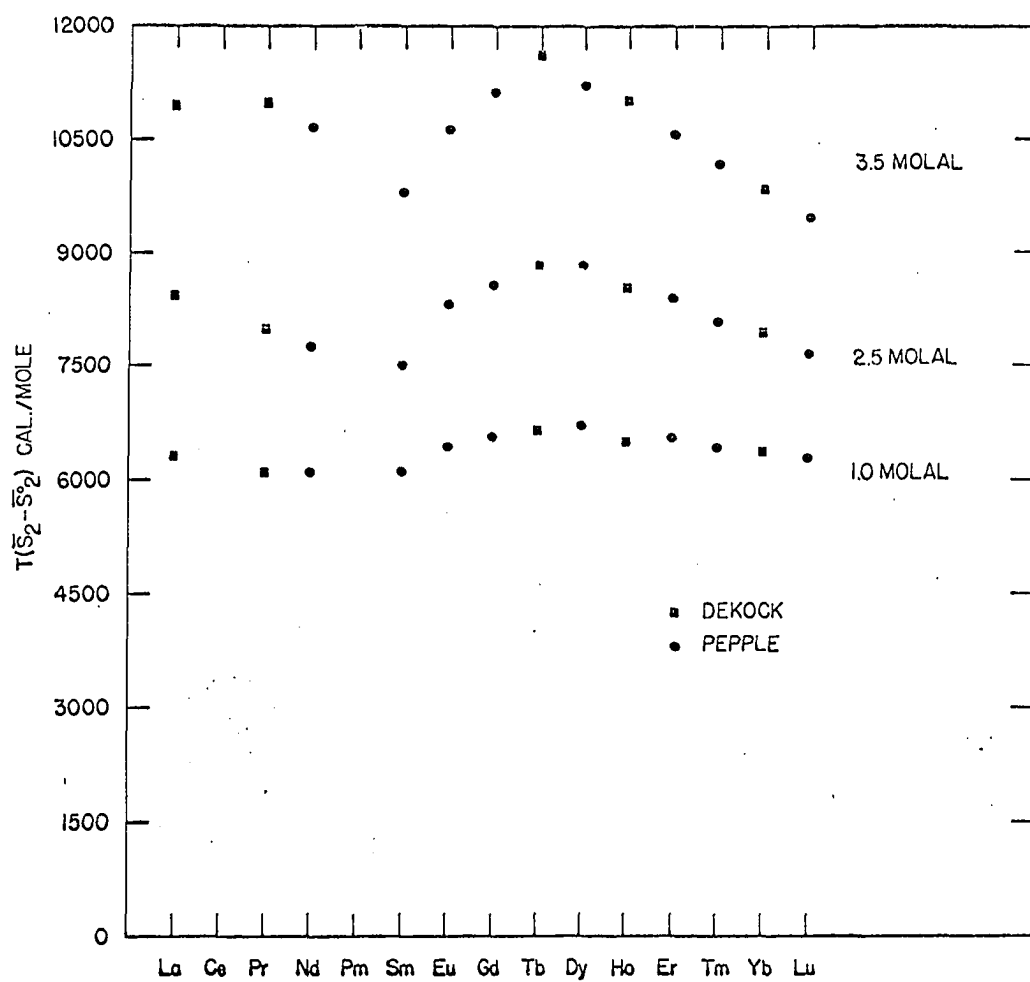
Figure 12. Relative partial molal excess entropies of the
solute in thirteen aqueous rare-earth chloride
solutions at three values of m at 25°C.
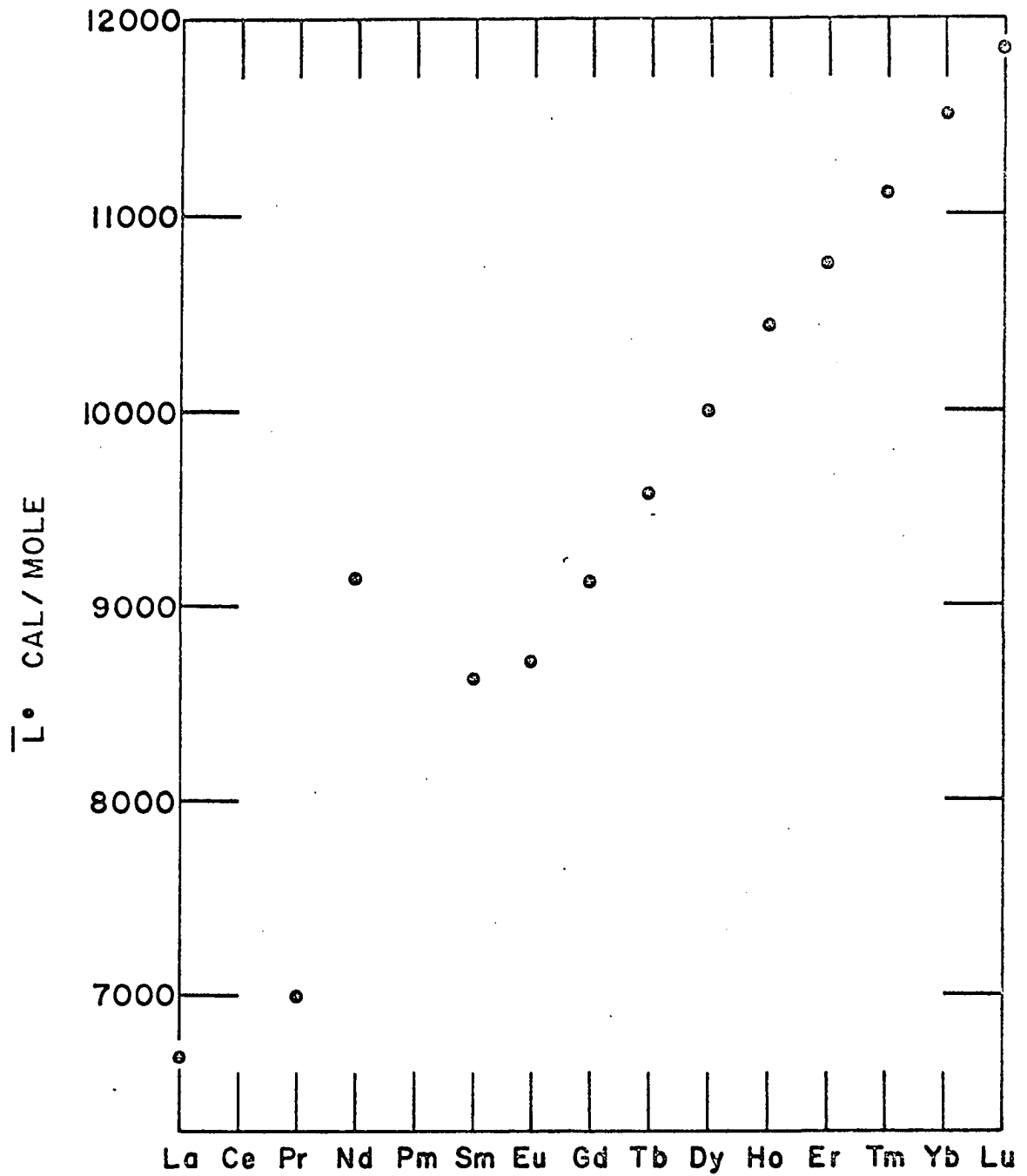
Figure 13. Relative molar heat contents of thirteen hydrated rare-earth chlorides at 25°C.

was assumed for the limiting slope of the $\overline{P}_i$ curves, so the total error in the $\overline{P}_i$ expressions is taken up by the uncertainties in the B coefficients. From the observed scatter in the $\overline{P}_i$ graphs it is unlikely that any of the B coefficients are in error more than 1500 units. An uncertainty of $\pm$ 1500 units in the B coefficients of the $\overline{P}_i$ expressions contributes an uncertainty of about 5 calories per mole to the $\emptyset_L$ values.

The $\overline{L}$ and $T(\overline{S} - \overline{S}^0)$ values are calculated through differentiation of the empirical polynomial expressions for the $\emptyset_L$ data. The least squares polynomials fit the $\emptyset_L$ data with a standard deviation of less than 9 calories per mole. It is difficult to estimate the errors introduced by differentiating these polynomials, but it is unlikely that this step contributes relative errors greater than 1 per cent to the $\overline{L}$ and $T(\overline{S} - \overline{S}^0)$ quantities.

The relative uncertainties in the experimental heats of solution of the rare-earth chloride hydrates are $\pm$ 0.3 per cent or less. An additional relative error of 0.1 per cent must be added on, due to the uncertainty of the composition of the hydrate samples, to give a total relative uncertainty in the heat of solution results of $\pm$ 0.4 per cent.

Eberts (5) measured the heat of solution of $NdCl_3 \cdot 6H_2O$ and Csejka (2) measured the heat of solution of $DyCl_3 \cdot 6H_2O$. Both of these measurements were carried out with an isothermal solution calorimeter. Eberts and Csejka estimated their relative errors to be $\pm$ 1.0 per cent, and within these limits

their results are in agreement with the results from this research. Flynn (8) measured the heats of solution of $LaCl_3 \cdot 7H_2O$, $PrCl_3 \cdot 7H_2O$, $SmCl_3 \cdot 6H_2O$, $GdCl_3 \cdot 6H_2O$, $ErCl_3 \cdot 6H_2O$, and $YbCl_3 \cdot 6H_2O$ and reported results which differ from the results of this research by an average of $\pm$ 5 per cent for the above six salts. Flynn measured the heats of solution of these hydrates with a calorimeter which was designed to measure the very much more exothermic heats of solution of the anhydrous rare-earth chlorides. It is felt that the differences between the results of this research and the results reported by Flynn can be attributed to the fact that he was measuring heats approximately one-fifth the size for which the apparatus was designed, and that consequently the relative errors in his hydrate experiments were about five times larger than his usual errors.

VIII. DISCUSSION AND SUMMARY

Values of $\overline{P}_i$ were determined in this research over the concentration range $m^{1/2} = 0.03$ to $m^{1/2} = 0.08$ for aqueous $NdCl_3$, $SmCl_3$, $EuCl_3$, $GdCl_3$, $DyCl_3$, $ErCl_3$, $TmCl_3$, and $LuCl_3$ solutions. The $\overline{P}_i$ data for each of the eight salts fell, within experimental error, on a linear curve which extrapolated to within about 5 per cent of the Debye-Hückel limiting law value at infinite dilution. In view of the inherent uncertainties in $\overline{P}_i$ these results constitute an excellent confirmation of the Debye-Hückel limiting law for 3-1 electrolytes.

The intercept value for all the $\overline{P}_i$ curves was set at the theoretical value to eliminate small differences due to uncertainties in the data and in the extrapolations. The B parameters in the $\overline{P}_i$ equations ranged approximately between 13000 and 16000 with an estimated 10 per cent uncertainty. The values of the B coefficients for the $\overline{P}_i$ expressions determined in this research fell within experimental error of the B coefficient values determined by Spedding and coworkers (50, 51b) for $NdCl_3$, $SmCl_3$, $GdCl_3$, $DyCl_3$, and $TmCl_3$. Their values for the B coefficients for $LaCl_3$, $PrCl_3$, $TbCl_3$, $HoCl_3$, and $TbCl_3$ also fell within the previously mentioned limits. This means that, within the accuracy which the parameters were determined, the curves for the different rare-earth chlorides are indistinguishable below $m^{1/2} = 0.08$. It will be seen later that the trend in the $\emptyset_L$ values across the rare-earth series at fixed

concentrations can be explained by systematic variations in the hydrated radii of the ions. It would seem surprising if a similar regular trend was not followed in the very dilute solutions.

In the earlier investigations of the $\bar{P}_i$ behaviour of the rare-earth chlorides considerable emphasis was put on collecting points at the extreme lower end of the concentration range, between $m^{1/2} = 0.01$ and $m^{1/2} = 0.03$. The relative errors in the $\bar{P}_i$ values become extremely large at these low concentrations, but except for $ErCl_3$ and $YbCl_3$ the $\bar{P}_i$ values from this region appeared to fall randomly about the linearly extrapolated curves. The $\bar{P}_i$ values for $ErCl_3$ and $YbCl_3$ take apparent downturns in the region of $m^{1/2} = 0.03$. The $\bar{P}_i$ behaviour of $YbCl_3$ was redetermined by DeKock (4) who concluded that the downturn was real, although the magnitude of the downturn was not much larger than the probable experimental error. Above $m^{1/2} = 0.03$, however, both the $ErCl_3$ and the $YbCl_3$ data appear to conform to the Debye-Hückel limiting law behaviour.

It is unlikely that these downturns can be accounted for by the dissociation of rare-earth-chloride complexes. The stability constants for the formation of the first rare-earth-chloride complex are of the order of unity at such extremely low concentrations and only a very small number of moles of the rare-earth ions would be complexed. In any event the complexed fraction would decrease as the rare-earth concentration decreased and the $\bar{P}_i$ values would tend towards rather than away

from the limiting law behaviour.

The equivalence pH of a rare-earth chloride solution rises as the concentration decreases. This suggests the possibility of the downturns in the $\bar{P}_i$ curves being due to some extraneous pH dependent reaction.

The rare-earth chloride solutions and the water into which they were diluted were in equilibrium with the atmosphere. It is possible that the downturn in the $\bar{P}_i$ curves is due to the formation of complexes between the rare-earth ions and carbon dioxide absorbed from the air. The amount of the carbon dioxide absorbed from the air and the extent of the complexing would both be pH dependent, and would both increase with rising pH. Carbon dioxide would be expected to complex to the highest degree with the light rare-earths, which are the most basic members of the series.

The heavy rare-earths are the most acidic and therefore have the highest hydrolysis stability constants. Frolova et al. (14) reported the logarithms of the stability constants for the formation of the first hydrolysis complexes according to equation 5.1 to be 8.01 for Er^{3+}, 8.05 for Tm^{3+}, and 8.08 for Lu^{3+} at an ionic strength of 0.3 molar. Using the value for Er^{3+} it was calculated that the ratio of the hydrolyzed to the nonhydrolyzed rare-earth ion increases from 7×10^{-3} at $m^{1/2} = 0.03$, to 17×10^{-3} at $m^{1/2} = 0.01$. The downturn in the $\bar{P}_i$ curve for $ErCl_3$ amounts to a lowering of the heat of dilution by approximately 40 calories per mole between these two

concentrations. A heat of formation of 4.0 kilocalories per mole for the hydrolysis complex could thus account for the observed downturn in the $\bar{P}_i$ curve.

The relative extent of both carbon dioxide complex formation and hydrolysis complex formation would increase as the rare-earth concentration decreased. Neither of these explanations suggest an obvious reason for why the downturn is seen only for $ErCl_3$ and $YbCl_3$. If this behaviour is due either to one of these reactions or to some other extraneous reaction similar downturns would be expected to show up at lower concentrations for each of the rest of the rare-earths. Unfortunately the relative error in $\bar{P}_i$ below $m^{1/2} = 0.03$ is extremely large and these downturns could easily be obscured.

The effects of these downturns, whatever the cause, can be eliminated from the $\emptyset_L$ curves by extrapolating the $\bar{P}_i$ data from the concentration regions where the limiting law behaviour is apparently being followed. This puts $ErCl_3$ and $YbCl_3$ on the same regular basis as the rest of the rare-earth chlorides and, for the sake of comparisons across the series, does not make the $\emptyset_L$ values of $ErCl_3$ and $YbCl_3$ appear anomalously low.

The $\emptyset_L$ curves for the rare-earth chlorides maintain the same relative order through the entire concentration range. Figure 5 shows a plot of $\emptyset_L$ versus $m^{1/2}$ for thirteen rare-earth chlorides and Figure 6 shows a plot of $\emptyset_L$ versus rare-earth at three molalities.

The trend in $\emptyset_L$ across the rare-earth series is systematic

but it does not appear that the $\emptyset_L$ values bear a simple relationship to the rare-earth ionic radii (which decrease monotonically across the series). The trend observed is similar to that observed by Spedding, Pikal, and Ayers (53) in the values of $\emptyset_V{}^o$, the apparent molal volume at infinite dilution, of the rare-earth chlorides. They observed that the $\emptyset_V{}^o$ values decreased from La to Nd, increased to Tb, and decreased through the rest of the series. This trend was interpreted as being due to the effect of the decreasing rare-earth ionic radii on the primary hydration spheres of the rare-earth ions. The volumes from La to Nd and from Tb to Yb show regular decreases caused by increasing electrostriction of the primary hydration spheres around the ions. The increase in volume between Nd and Tb is attributed to a coordination number change; a decrease in the number of water molecules in the primary hydration sphere of the rare-earth ions. Since the total volume increase is not abrupt the assumption is made that an equilibrium exists in solution between the two hydration forms.

An analogous trend has been observed for the heats of formation of several chelates with the rare-earth ions. Mackey, Powell, and Spedding (35) observed this trend for EDTA complexes, Grenthe (19, 20) for diglycollate and dipicolinate complexes, and Edelin de Praudiere and Stavely (6) for the nitrilotriacetate complexes. These authors all agree that the trend shown by the heats of formation of the 1:1 complexes of these chelates across the rare-earth series cannot be explained

by ligand field effects on the 4f electrons, but is probably
due to a change in the hydration number of the rare-earth ions
in the middle of the series. The results of Jones (30) on the
heat capacities and of Pikal (40) on the viscosities of aqueous
rare-earth chloride solutions are also compatible with a gradual
decrease in the average number of primary hydration waters
midway through the series. The idea of two primary coordination
forms being possible is supported by the structural studies of
Helmholtz (28) who reported a nine-coordinated $Nd(BrO_3)_3 \cdot 9H_2O$
and of Marezio et al. (36) who reported an eight-coordinated
$GdCl_3 \cdot 6H_2O$.

The extended Debye-Hückel theory predicts (equation 2.11)
that $\emptyset_L$ will vary inversely with a^o, the mean distance of
closest approach of the ions. The $\emptyset_L$ values shown in Figure 6
are all at concentrations much higher than the range of validi-
ty of the Debye-Hückel theory, but it is expected that the
inverse proportionality relationship between the distance of
closest approach of the ions and $\emptyset_L$ should be approximately
maintained.

The ion-size parameter will depend upon the total extent
of hydration of the rare-earth ions. The average hydrated
radii of the rare-earth ions will change in exactly an opposite
manner from the primary hydration sphere radii. That is to
say, as the primary hydration sphere radii decrease, as from La
to Nd and from Tb to Lu, the electric fields around the primary
hydrate species will increase and these ions will exert an

increasingly stronger influence on the surrounding waters in the solution. The hydrated ionic radii will therefore increase from La to Nd and from Tb to Lu, and by the same argument they will decrease between Nd and Tb. An inverse proportionality between these hydrated radii and the apparent molal heat contents would produce the trend in the $\emptyset'_L$ values observed in Figure 6.

The relative apparent molal heat content curves, shown in Figure 5 as a function of $m^{1/2}$, can be conveniently discussed in terms of three general regions. In the lowest region, below $m^{1/2} = 0.1$, the $\emptyset_L$ values rise rapidly as predicted by the Debye-Huckel theory. In the intermediate region the $\emptyset_L$ values increase less rapidly and become approximately linear between $m^{1/2} = 0.3$ and $m^{1/2} = 0.8$. In the highest region, above $m^{1/2} = 1.0$, the $\emptyset_L$ values rise rapidly. It is an interesting feature of these $\emptyset_L$ values that when they are plotted versus $m^{3/2}$ the values between 1.25 molal and saturation lie on a straight line.

Goto and Smutz (18) report a stability constant of 1.60 ± 0.03 at an ionic strength of one-molal for the first chloride complexes of the light rare-earths. DeKock (4) measured the heat of complexing of La^{3+}, Tb^{3+}, and Yb^{3+} in one-molal hydrochloric acid solutions versus one-molal perchloric acid solutions and reported a result of $\Delta H = -1.5 \pm 0.1$ kilocalories per mole for the heat of formation of the first chloride complex RCl^{2+} for each of the three ions. Using these results it was calculated that approximately one fourth of the

heat evolved in the dilution of one mole of rare-earth chloride from $m^{1/2} = 0.6$ to $m^{1/2} = 0.4$ is cancelled by the dissociation of the RCl^{2+} complex. This effect thus accounts in part for the decreased slope of the $\emptyset_L$ curves across the intermediate concentration region.

At a concentration of $m^{1/2} = 1.0$ there are only 55 molecules of water for every rare-earth ion and three chloride ions, and by $m^{1/2} = 2.0$ this ratio decreases to 14 to 1. The strong decrease in the activity of the water in rare-earth chloride solutions above one molal suggests that hydration effects become important at high concentrations. The evolution of heat from the fulfillment of the hydration requirements of the rare-earth ions probably accounts for a large share of the increase in the slope of the $\emptyset_L$ curves above one molal.

At high concentrations it is likely that higher order chloride complexes, RCl_2^+ or RCl_3, are formed in significant amounts. It is also likely that the formation of inner-sphere complexes with one or more chloride ions replacing primary hydration waters may become favored. This latter possibility is given support by Marezio et al. (36) who found two chloride ions adjacent to the rare-earth ion in $GdCl_3 \cdot 6H_2O$. The dissociation of the inner sphere or higher order complexes would probably be exothermic reactions and could contribute significantly to the increase in $\emptyset_L$.

The trends shown by the relative partial molal heat contents $\bar{L}_2$ and the relative partial molal excess entropies

$(\overline{S}_2 - \overline{S}_2{}^{\circ})$ of the rare-earth chlorides, shown respectively in Figures 9 and 12, are compatible with the hydration-change explanation given for the relative apparent molal heat contents. Exactly the same argument can be made to explain the variations in $\overline{L}_2$ across the rare-earth series as was made in explaining the variations in $\emptyset_L$.

According to Friedman (13) negative changes in the partial molal excess entropy of the solvent (and hence positive entropy changes of the solute) reflect the loss of entropy of the solvent molecules in the electric field of the ions. He also states that the electric field from an ion should become more effective in decreasing the entropy of the solvent as the solution concentration decreases. This accounts for the rapid increase in $(\overline{S}_2 - \overline{S}_2{}^{\circ})$ in the limiting law region. Frank and Robinson (12) interpret the relative partial molal entropies in terms of structure making and structure breaking effects on the structure of the water. They attribute positive increases in $(\overline{S}_1 - \overline{S}_1{}^{\circ})$ to breakdown of the water structure by ions which cannot fit into the structure. The behaviour of the $T(\overline{S}_1 - \overline{S}_1{}^{\circ})$ curves, shown for $SmCl_3$ in Figure 10, can be explained on the basis of the ordering effects of the rare-earth ions. The rare-earth ions and the chloride ions break down the water structure, but the hydrate waters become ordered to a higher degree around the rare-earth ions than they were in pure water. As the rare-earth concentration increases an average water molecule is exposed to stronger electric fields from the ions

and this accounts for the continual decrease in the $T(\bar{S}_1 - \bar{S}_1^{\,o})$ values. Entropy changes due to ion complexing and due to changes in the degree of hydrogen bonding of the solvent will also contribute to the partial molal excess entropy values.

At any given concentration the trend in the $T(\bar{S}_2 - \bar{S}_2^{\,o})$ values across the rare-earth series can be interpreted in terms of the ordering effects taking place in the hydrated ions. Across the series from La to Nd and from Tb to Yb the increasing electric field of the rare-earth ions will cause the primary hydration sphere and the surrounding solvent molecules to be increasingly highly ordered. Thus the relative partial molal excess entropy of the solute will decrease across these two portions of the series. From Nd to Tb the average primary hydrated radii increase due to the shift in the equilibrium between the higher and lower coordinated hydration forms. The primary hydration sphere waters and the surrounding waters are bound in a decreasingly strong electric field and the relative excess entropy values of the solute become more positive across this region.

Above two molal the $\bar{L}_2$ and $T(\bar{S}_2 - \bar{S}_2^{\,o})$ values increase more rapidly for $PrCl_3$ and $NdCl_3$ than for the rest of the series. This behaviour can be explained in terms of a concentration dependent primary hydration shift. As the competition for the water increases at high concentrations it could become energetically favorable for some of the ions to shift to the low-coordinated primary hydration form. Saeger (45) and Jones (30)

have proposed such a hydration change to explain, respectively, the apparently anomalous behaviour of the partial molal volume and partial molal heat capacity of $NdCl_3$.

Figure 13 shows a plot of $\bar{L} \cdot$, the relative molar heat content, or the heat of solution with respect to infinite dilution, of the hydrated rare-earth chlorides. The values for $TbCl_3 \cdot 6H_2O$ and $HoCl_3 \cdot 6H_2O$ are taken from the results of DeKock (4). The experimental values of $\bar{L} \cdot$ are listed in Table 24.

The two least exothermic heat of solution values are those of $LaCl_3 \cdot 7H_2O$ and $PrCl_3 \cdot 7H_2O$. These were the only heptahydrate salts which were measured; at $25^{\circ}C$. the remaining members of the series crystallize in their most stable forms as hexahydrates.

Considering each rare-earth chloride hexahydrate with respect to its solution reference state, $SmCl_3 \cdot 6H_2O$ has the least exothermic heat of solution. The heats of solution become more exothermic in regular increments from $EuCl_3 \cdot 6H_2O$ through $LuCl_3 \cdot 6H_2O$. From Sm through Lu the increasing molar heat contents of the hydrated crystals can be correlated with their decreasing molar volumes[1]. The rise in the molar heat contents can be interpreted as a measure of the energy taken up by the crystals due to the stronger interactions between the ions as they pack more closely together. The relatively high

---

[1]Spedding, F. H. and Mohs, M. A., Ames Laboratory of the A.E.C., Ames, Iowa. Molar volumes of the rare-earth chloride hydrates. Private communication. 1966.

value of the molar heat content of $NdCl_3 \cdot 6H_2O$ can be attributed to the equilibrium between the two primary hydration forms in solution. In the crystal the Nd^{3+} ion exists exclusively in the eight-coordinated form and a shift of a fraction of the ions to a higher coordinated form in solution would be expected to be accompanied by an exothermic heat effect.

The reaction of a crystal with water to form a saturated solution is an equilibrium process and can be described for a rare-earth chloride system by equations 8.1 and 8.2.

$$RCl_3 \cdot nH_2O(c) + XH_2O(l) = RCl_3(sat.) \qquad (8.1)$$
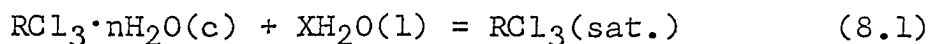
$$\Delta H_C = T\Delta S_C = \phi_L(sat.) - \overline{L} \cdot \qquad (8.2)$$

Values of ΔH_C are listed in Table 25 and are plotted versus rare-earth in Figure 14.

Reaction 8.2 reflects the entropy change for one mole of crystal plus X moles of water going to saturated solution. This suggests describing the entropy change for equation 8.1 in the following manner.

$$T\Delta S_C = T(\overline{S}_2 - \overline{S}_2^{\,o})(sat.) + nT(\overline{S}_1 - \overline{S}_1^{\,o})(sat.)$$

$$+ XT(\overline{S}_1 - \overline{S}_1^{\,o})(sat.) - T(\overline{S} \cdot - \overline{S}_2^{\,o} - n\overline{S}_1^{\,o})$$

$$(8.3)$$

The terms in equation 8.3 can be rearranged and grouped to define the new quantity $T\Delta S_C'$, which represents the difference in entropy between the saturated solution and the crystal for

Table 25. Enthalpies of solution of the hydrated rare-earth chlorides in water at 25°C.

	$T\Delta S_c$ cal./mole	X	$T(\bar{S}_1-\bar{S}_1^o)$ (Sat.) cal./mole	$T\Delta S_c'$ cal./mole	$T(\bar{S}-\bar{S}_2^o-n\bar{S}_1^o)$ cal./mole
La	898	7.25	−284	2957	7185
Pr	493	7.27	−330	2892	7368
Nd	−1660	8.13	−330	1023	9440
Sm	−1495	9.24	−183	196	8966
Eu	−1427	9.47	−190	372	9358
Gd	−1551	10.16	−226	745	9301
Tb	−1698	9.54	−244	630	9776
Dy	−2004	9.29	−226	96	10140
Ho	−2353	9.03	−241	−177	10321
Er	−2611	8.68	−231	−606	10574
Tm	−2886	8.30	−238	−911	10694
Yb	−3118	7.87	−237	−1253	10919
Lu	−3318	7.45	−241	−1523	11021
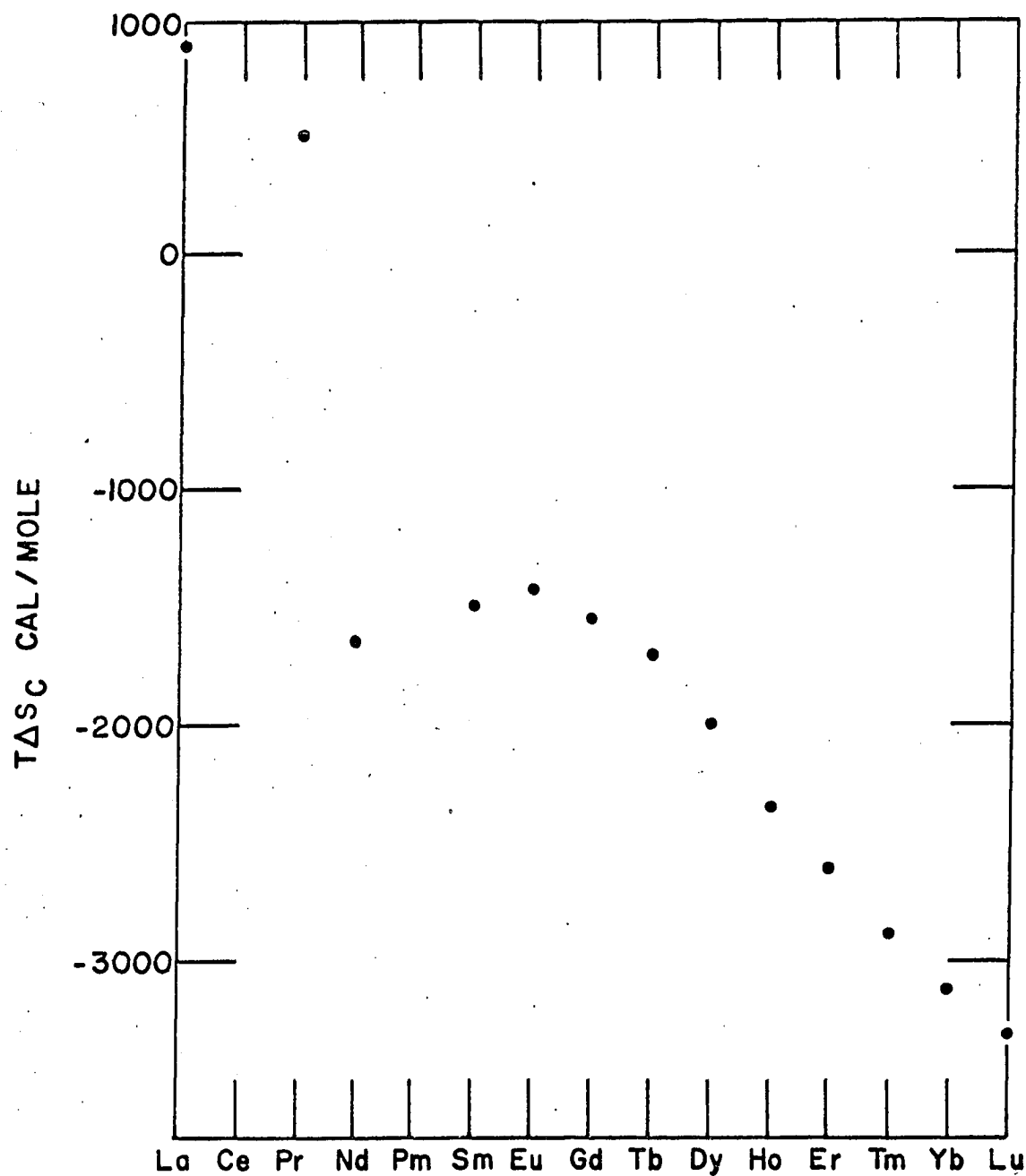
Figure 14. Enthalpies of solution of thirteen hydrated rare-earth chlorides in water at 25°C.

the unit (RCl_3 + nH_2O) where n is 6 or 7.

$$T \Delta S_C' = T\left[\overline{S}_2(\text{sat.}) - \overline{S}_2 \cdot\right] + nT\left[\overline{S}_1 (\text{sat.}) - \overline{S}_1 \cdot\right] \tag{8.4}$$

$$T \Delta S_C' = T \Delta S_C - XT(\overline{S}_1 - \overline{S}_1^{\,0})(\text{sat.}) \tag{8.5}$$

The quantity $T(\overline{S}_1 - \overline{S}_1^{\,0})$ is the relative partial molal excess entropy of the solvent in the saturated solution and is tabulated in Table 25 along with values of the rest of the terms in the previous equations.

The values of $T \Delta S_C'$ are negative from Ho through Lu. An order-disorder interpretation of these entropy values leads to the conclusion that the (RCl_3 + nH_2O) units are more ordered in a saturated solution than in a crystal. This possibility seems contrary to experience but it cannot be ruled out until the microscopic state of the system is better understood. The hydrated waters in a crystal have no neighbors to which they can hydrogen bond. Since these waters could be hydrogen bonded in the solution, it is possible that they could gain some degrees of freedom in passing to the crystalline state.

The molar entropies of the (RCl_3 + nH_2O) units can be calculated with respect to infinite dilution for each rare-earth for which the relative partial molal excess entropies of dilution of the rare-earth chlorides are known.

$$T\left[\overline{S} \cdot - \overline{S}_2^{\,0} - n\overline{S}_1^{\,0}\right] = \left[\overline{S}_2(\text{sat.}) - \overline{S}_2^{\,0}\right] +$$

$$nT\left[\overline{S}_1(\text{sat.}) - \overline{S}_1^{\,0}\right] - T \Delta S_C' \tag{8.6}$$

The values calculated from equation 8.6 are listed in Table

25. When the heat capacities of the hydrated crystals are

measured from sufficiently low temperatures to room temperature

it will be possible to calculate the absolute entropies of the

$(RCl_3 + nH_2O)$ units in their infinitely dilute reference states.

In summary, the heats of dilution of aqueous $NdCl_3$, $SmCl_3$,

$EuCl_3$, $GdCl_3$, $DyCl_3$, $ErCl_3$, $TmCl_3$, and $LuCl_3$ solutions were

measured from zero concentration to saturation at $25^{\circ}C$. The

heats of solution of $LaCl_3 \cdot 7H_2O$, $PrCl_3 \cdot 7H_2O$, $NdCl_3 \cdot 6H_2O$,

$SmCl_3 \cdot 6H_2O$, $EuCl_3 \cdot 6H_2O$, $GdCl_3 \cdot 6H_2O$, $DyCl_3 \cdot 6H_2O$, $ErCl_3 \cdot 6H_2O$,

$TmCl_3 \cdot 6H_2O$, $YbCl_3 \cdot 6H_2O$, and $LuCl_3 \cdot 6H_2O$ in water at $25^{\circ}C$. were

also measured.

Empirical least square equations were determined from

these data, using an IBM 360 computer, to express the relative

apparent molal heat contents, $\emptyset_L$, as functions of $m^{1/2}$. The

relative partial molal heat contents of the solvent, $\bar{L}_1$, and of

the solute, $\bar{L}_2$, were calculated from these empirical ex-

pressions. The relative partial molal entropies of dilution of

the solvent, $T(\bar{S}_1 - \bar{S}_1^{\,\circ})$, and of the solute, $T(\bar{S}_2 - \bar{S}_2^{\,\circ})$, were

determined from the $\bar{L}_1$ and $\bar{L}_2$ values and from the activity

coefficient data for these electrolytes. Values of $\bar{L}_1$, $\bar{L}_2$,

$T(\bar{S}_1 - \bar{S}_1^{\,\circ})$, and $T(\bar{S}_1 - \bar{S}_1^{\,\circ})$ were calculated at rounded concen-

trations.

The data indicate that these eight rare-earth chlorides

obey the Debye-Hückel limiting law in aqueous solution in the

concentration range 0.001 to 0.007 molal. The data for the

more concentrated rare-earth chloride solutions can be explained

in terms of two series within the rare-earths. These two series

have different coordination numbers in solution. The heavy

rare-earths, Tb through Lu, exist in the lower coordinated form.

For the light rare-earths there is an equilibrium between the

two forms, with the higher coordinated form being most favored

for La and Nd. Above 2.0 molal the data for $NdCl_3$ indicate

that an equilibrium favoring the formation of the lower co-

ordinated form becomes important.

IX. BIBLIOGRAPHY

1. Bjerrum, N., _Kgl. Danske Videnske. Selskab._, _7_, No. 9 (1926). Original available but not translated; cited in Harned, H. S. and Owen, B. B., "The physical chemistry of electrolytic solutions", 3rd. ed., page 70, Reinhold Publishing Corporation, New York, N.Y., 1958.

2. Csejka, David A., "Some thermodynamic properties of aqueous rare-earth chloride solutions", Unpublished Ph.D. thesis, Library, Iowa State University of Science and Technology, Ames, Iowa, 1961.

3. Debye, P. and Hückel, E., _Physik. Z._, _24_, 185 (1923).

4. DeKock, Carroll W., "Heats of dilution of some aqueous rare-earth chloride solutions at 25°C", Unpublished Ph.D. thesis, Library, Iowa State University of Science and Technology, Ames, Iowa, 1965.

5. Eberts, Robert E., "Relative apparent molal heat contents of some rare-earth chlorides and nitrates in aqueous solutions", Unpublished Ph.D. thesis, Library, Iowa State University of Science and Technology, Ames, Iowa, 1957.

6. Edelin De La Praudiere, P. L. and Stavely, L. A. K., _J. Inorg. Nucl. Chem._, _26_, 1713 (1964).

7. Eigen, M. and Wicke, E., _J. Phys. Chem._, _58_, 702 (1954).

8. Flynn, James P., "Heats of solution and related thermochemical properties of some rare-earth metals and chlorides", Unpublished Ph.D. thesis, Library, Iowa State University of Science and Technology, Ames, Iowa, 1953.

9. Foulk, C. W. and Hollingsworth, M., _J. Am. Chem. Soc._, _45_, 1220 (1923).

10. Fowler, R. H., _Trans. Faraday Soc._, _23_, 434 (1927).

11. Fowler, R. and Guggenheim, E. A., "Statistical thermodynamics", Cambridge University Press, Cambridge, England, 1960.

12. Frank, H. S. and Robinson, A. L., _J. Chem. Phys._, _8_, 933 (1940).

13. Friedman, H. L., _J. Chem. Phys._, _32_, 1351 (1960).

14. Frolova, U. K., Kumok, V. N. and Serebrennikov, V. V., Izv. Vysshikh Uchebn. Zavedenii, Khim. i Khim. Tekhnol., 9, 176 (1966). Original not available for examination; abstracted in Chemical Abstracts, 65, 9816b (1966).

15. Fuoss, R. M. and Krauss, C. A., J. Am. Chem. Soc., 55, 2387 (1933).

16. Fuoss, R. M. and Krauss, C. A., J. Am. Chem. Soc., 57, 1 (1935).

17. Glueckauf, E., Trans. Faraday Soc., 51, 1235 (1955).

18. Goto, T. and Smutz, M., J. Inorg, Nucl. Chem., 27, 663 (1965).

19. Grenthe, I., Acta Chem. Scand., 17, 2487 (1963).

20. Grenthe, I., Acta Chem. Scand., 18, 293 (1964).

21. Gronwall, T. H., La Mer, V. K. and Greiff, L. J., J. Phys. Chem., 35, 2245 (1931).

22. Gucker, F. T., Jr., Pickard, H. B. and Planck, R. W., J. Am. Chem. Soc., 61, 459 (1939).

23. Guggenheim, E. A., Trans. Faraday Soc., 55, 1714 (1959).

24. Gulbransen, E. A. and Robinson, A. L., J. Am. Chem. Soc., 56, 2637 (1934).

25. Hale, J. D., Izatt, R. M. and Christensen, J. J., J. Phys. Chem., 67, 2605 (1963).

26. Harned, H. S., J. Am. Chem. Soc., 57, 1865 (1935).

27. Harned, Herbert S. and Owen, Benton B., "The physical chemistry of electrolytic solutions", 3rd. ed., Reinhold Publishing Corporation, New York, N.Y., 1958.

28. Helmholtz, L., J. Am. Chem. Soc., 61, 1544 (1939).

29. Hückel, E., Physik. Z., 26, 93 (1925).

30. Jones, Kenneth C., "Partial molal heat capacities of some aqueous rare-earth chloride solutions at 25°C", Unpublished Ph.D. thesis, Library, Iowa State University of Science and Technology, Ames, Iowa, 1965.

31. Kirkwood, J. G., J. Chem. Phys., 2, 767 (1934).

32. Kirkwood, J. G. and Poirier, J. C., J. Phys. Chem., 58, 591 (1954).

33. Kramers, H. A., Proc. Acad. Sci. Amsterdam, 30, 145 (1927).

34. Lange, E., "Heats of dilution of dilute solutions of strong and weak electrolytes". In Hamer, W. J., eds. "The structure of electrolytic solutions", pages 135-151, John Wiley and Sons, Inc., New York, N.Y., 1959.

35. Mackey, J. L., Powell, J. E. and Spedding, F. H., J. Am. Chem. Soc., 84, 2047 (1962).

36. Marezio, M., Plettinger, H. A. and Zachariasen, W. H., Acta Cryst., 14, 234 (1961).

37. Naumann, Alfred W., "Heats of dilution and related thermo-dynamic properties of aqueous neodymium and erbium chloride solutions", Unpublished Ph.D. thesis, Library, Iowa State University of Science and Technology, Ames, Iowa, 1956.

38. Onsager, L., Chem. Rev., 13, 73 (1933).

39. Petheram, Harry H., "Osmotic and activity coefficients of some aqueous rare-earth chloride solutions at 25°C", Unpublished Ph.D. thesis, Library, Iowa State University of Science and Technology, Ames, Iowa, 1963.

40. Pikal, Michael J., "Apparent molal volumes and viscosities of some aqueous rare-earth chloride solutions at 25°C", Unpublished Ph.D. thesis, Library, Iowa State University of Science and Technology, Ames, Iowa, 1966.

41. Powell, Jack E., "Separation of rare-earths by ion ex-change", In Spedding, F. H. and Daane, A. H., eds. "The rare-earths", pages 55-73, John Wiley and Sons, Inc., New York, N.Y., 1961.

42. Robinson, A. L. and Wallace, W. E., J. Am. Chem. Soc., 63, 1582 (1942).

43. Robinson, R. A. and Stokes, R. H., "Electrolytic so-lutions", 2nd ed., Butterworths Scientific Publications, London, England, 1959.

44. Rossini, Frederick D., Wagman, Donald D., Evans, William H., Levine, Samuel and Jaffe, Irving, U. S. National Bureau of Standards Circular 500 (1952).

45. Saeger, Victor W., "Some physical properties of rare-earth chlorides in aqueous solution", Unpublished Ph.D. thesis, Library, Iowa State University of Science and Technology, Ames, Iowa, 1960.

46. Salman, B. C. L. and White, A. G., J. Chem. Soc., (London), 3197 (1957).

47. Scatchard, G., Chem. Rev., 19, 309 (1936).

48. Skinner, H. A., "Experimental thermochemistry", Vol. 2, Interscience Publishers Inc., New York, N.Y., 1962.

49. Spedding, F. H. and Atkinson, Gordon, "Properties of rare-earth salts in electrolytic solutions", In Hamer, Walter J., ed., "The structure of electrolytic solutions", pages 319-339, John Wiley and Sons, Inc., New York, N.Y., 1959.

50. Spedding, F. H., Csejka, D. A. and DeKock, C. W., J. Phys. Chem., 70, 2423 (1966).

51a. Spedding, F. H. and Jones, K. C., J. Phys. Chem., 70, 2450 (1966).

51b. Spedding, F. H., Naumann, A. W. and Eberts, R. E., J. Am. Chem. Soc., 81, 23 (1959).

52. Spedding, F. H. and Pikal, M. J., J. Phys. Chem. 70, 2430 (1966).

53. Spedding, F. H., Pikal, M. J. and Ayers, B. O., J. Phys. Chem., 70, 2440 (1966).

54. Stokes, R. H. and Robinson, R. A., J. Am. Chem. Soc., 70, 1870 (1948).

55. Sturtevant, J. M., "Calorimetry", in Weissburger, Arnold, ed., "Technique of organic chemistry", 3rd ed., Vol. 1, Part 1, pages 523-655, Interscience Publishers, Inc., New York, N.Y., 1959.

56. Swietoslawski, W., "Microcalorimetry", Reinhold Publishing Corporation, New York, N.Y., 1946.

57. Vanderzee, C. E. and Swanson, J. A., J. Phys. Chem., 67, 2608 (1963).

58a. Vogel, Arthur II, "A text-book of quantitative inorganic analysis", 3rd ed., John Wiley and Sons, Inc., New York, N.Y., 1961.

58b. Washburn, E. W., "International critical tables of nu-
     merical data", McGraw Hill Book Co., New York, N.Y., 1930.

59. White, W. P., "The modern calorimeter", The Chemical Cata-
     log Company, Inc., New York, N.Y., 1928.

60. Wicke, E. and Eigen, M., $\underline{Z}$. Electrochem., $\underline{56}$, 551 (1952).

61. Wood, R. H. and Smith, R. W., $\underline{J}$. Phys. Chem., $\underline{69}$, 2974
     (1965).

62. Wyman, J. and Ingalls, E. N., $\underline{J}$. Am. Chem. Soc., $\underline{60}$, 1182
     (1938).

63. Young, T. F. and Groenier, W. L., $\underline{J}$. Am. Chem. Soc., $\underline{58}$
     187 (1936).

64. Young, T. F. and Seligmann, P., $\underline{J}$. Am. Chem. Soc., $\underline{60}$,
     2379 (1938).

65. Young, T. F. and Vogel, O. G., $\underline{J}$. Am. Chem. Soc., $\underline{54}$, 3030
     (1932).

66. Young, T. F., Wu, Y. C. and Krawetz, A. A., Discussions
     Faraday Soc., $\underline{24}$, 37 (1957).

X. ACKNOWLEDGEMENTS